Mid-IR lasers: Challenges Imposed by the Population Dynamics of the Gain System

Markus Pollnau

Integrated Optical MicroSystems Group

MESA+ Institute for Nanotechnology

University of Twente

Enschede, The Netherlands

m.pollnau@ewi.utwente.nl

Report Documentation Page

Form Approved
OMB No. 0704-0188

1. REPORT DATE **SEP 2010**	2. REPORT TYPE **N/A**	3. DATES COVERED **-**

4. TITLE AND SUBTITLE **Mid-IR lasers: Challenges Imposed by the Population Dynamics of the Gain System**	5a. CONTRACT NUMBER 5b. GRANT NUMBER 5c. PROGRAM ELEMENT NUMBER
6. AUTHOR(S)	5d. PROJECT NUMBER 5e. TASK NUMBER 5f. WORK UNIT NUMBER
7. PERFORMING ORGANIZATION NAME(S) AND ADDRESS(ES) **Integrated Optical MicroSystems Group MESA+ Institute for Nanotechnology University of Twente Enschede, The Netherlands**	8. PERFORMING ORGANIZATION REPORT NUMBER
9. SPONSORING/MONITORING AGENCY NAME(S) AND ADDRESS(ES)	10. SPONSOR/MONITOR'S ACRONYM(S) 11. SPONSOR/MONITOR'S REPORT NUMBER(S)

12. DISTRIBUTION/AVAILABILITY STATEMENT
Approved for public release, distribution unlimited

13. SUPPLEMENTARY NOTES
See also ADA564694. Mid-Infrared Fiber Lasers (Les fibres laser infrarouge moyen). RTO-MP-SET-171

14. ABSTRACT

15. SUBJECT TERMS

16. SECURITY CLASSIFICATION OF:			17. LIMITATION OF ABSTRACT	18. NUMBER OF PAGES	19a. NAME OF RESPONSIBLE PERSON
a. REPORT **unclassified**	b. ABSTRACT **unclassified**	c. THIS PAGE **unclassified**	**SAR**	**57**	

Outline

1. Introduction: Level scheme, spectroscopic processes
2. Erbium 3-µm fiber lasers: Depleting the lower laser level
3. The cascade-lasing regime
4. The lifetime-quenching regime
5. The energy-recycling regime
6. The thermal problem
7. Another cascade-lasing regime
8. Other 3-µm fiber laser
9. Conclusions

Lanthanide Ions in the Periodic System

1a	2a											3a	4a	5a	6a	7a	8a
H																	He
Li	Be											B	C	N	O	F	Ne
Na	Mg	3b	4b	5b	6b	7b	8b	8b	8b	1b	2b	Al	Si	P	S	Cl	Ar
K	Ca	Sc	Ti	V	Cr	Mn	Fe	Co	Ni	Cu	Zn	Ga	Ge	As	Se	Br	Kr
Rb	Sr	Y	Zr	Nb	Mo	Tc	Ru	Rh	Pd	Ag	Cd	In	Sn	Sb	Te	J	Xe
Cs	Ba	La	Hf	Ta	W	Re	Os	Ir	Pt	Au	Hg	Tl	Pb	Bi	Po	At	Rn
		↑	58 Ce	59 Pr	60 Nd	61 Pm	62 Sm	63 Eu	64 Gd	65 Tb	66 Dy	67 Ho	68 Er	69 Tm	70 Yb	71 Lu	
Fr	Ra	Ac	Lr	Rf	Db	Sg	Bh	Hs	Mt	Ds							
		↑	Th	Pa	U	Np	Pu	Am	Cm	Bk	Cf	Es	Fm	Md	No	Lw	

Lanthanide = 4f rare-earth ion, $_{57+n}$Ln [$_{54}$Xe $6s^2$ 5d $4f^n$ or $_{54}$Xe $6s^2$ $4f^{n+1}$]

Shielding of the 4f Sub-shell

1. Shielding vs. core electric charge by inner shells (1s, ..., 4d)

$\Rightarrow$ central-field approximation
(neglects perturbations within 4f sub-shell)

2. Shielding vs. interactions with host lattice
by outer 5s and 5p sub-shells

$\Rightarrow$ relatively small electron-phonon coupling

Energy Levels: Central Field Approximation

The energy of the 4f subshell can be calculated in the central field approximation.

This approach takes into account the electric field produced by the charge of the nucleus and the charges of the filled inner shells which shield the charge of the nucleus.

It neglects the coulomb interaction between electrons within the partially filled 4f subshell, their spin-orbit coupling, and the crystal field generated by the ligand ions in the host material.

Central-Field Approximation: Perturbations

1. a) **Non-centrosymmetric splitting (Coulomb interaction)**
   ⇒ total orbital angular momentum $\vec{L} = \sum \vec{\ell}$

   b) **Accordingly:**
   ⇒ total electron-spin momentum $\vec{S} = \sum \vec{s}$

2. **Spin-orbit coupling ("LS" coupling)**
   ⇒ total angular momentum $\vec{J} = \vec{L} + \vec{S}$
   lanthanides: intermediate coupling (*LS* / *jj*)

3. **Crystal-field splitting ("Stark effect")**
   ⇒ total magnetic dipole moment $\vec{m}_J$

Amounts of Splittings

1. Non-centrosymmetric splitting ~ 10000 cm^{-1}
2. Spin-orbit splitting ~ 1000 cm^{-1}
3. Crystal-field splitting ~ 100 cm^{-1}

Unit (cm^{-1}) : photon energy $E = hc / \lambda \propto 1 / \lambda$

5000 cm^{-1} = 2 μm

10000 cm^{-1} = 1 μm

20000 cm^{-1} = 500 nm

Partial Energy-Level Scheme of Er^{3+}

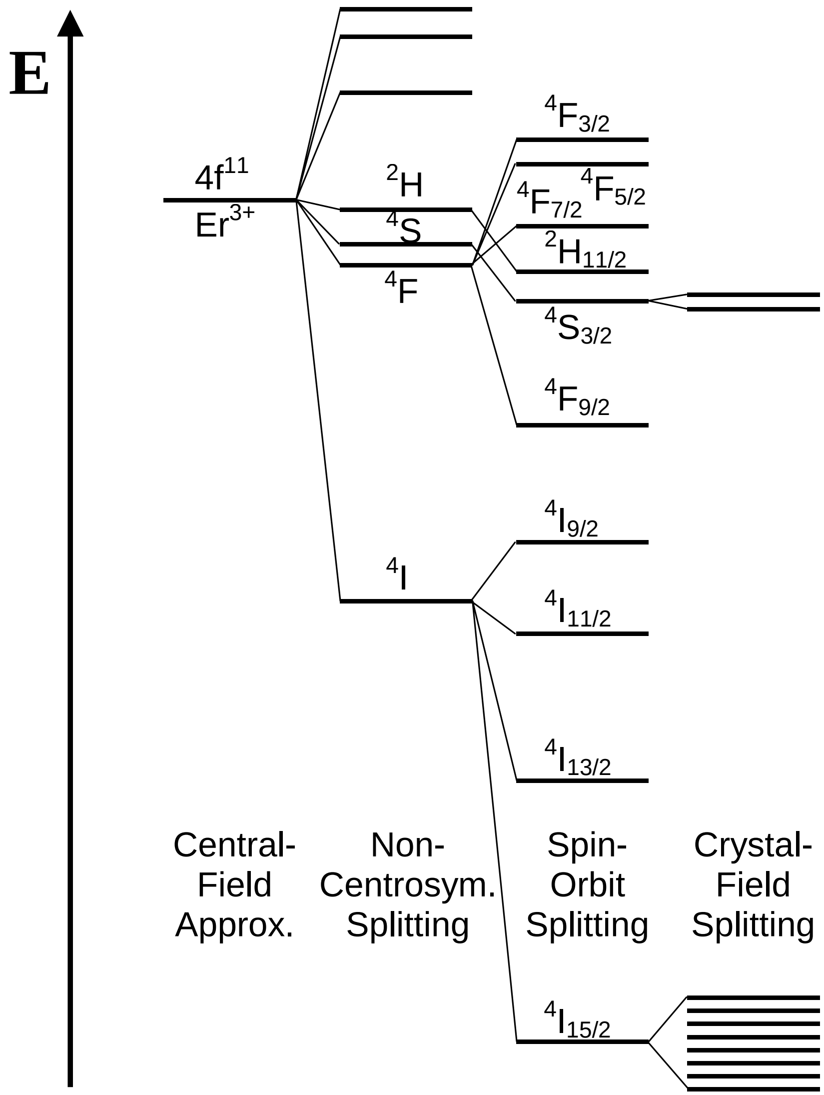

MESA+ Institute for Nanotechnology

m.pollnau@ewi.utwente.nl

Integrated Optical MicroSystems (IOMS)

University of Twente
Enschede - The Netherlands

Boltzmann Factors

At room temperature (300 K), $k_B T$ = 200 cm^{-1} is in the order of the energy splitting within a crystal-field multiplet

⇒ Boltzmann distribution of excitation energy within each crystal-field multiplet $^{2S+1}L_J$

$$f_i = \frac{\exp\left[\left(E_1 - E_i\right)/\left(k_B T\right)\right]}{\sum_i \left\{\exp\left[\left(E_1 - E_i\right)/\left(k_B T\right)\right]\right\}}$$

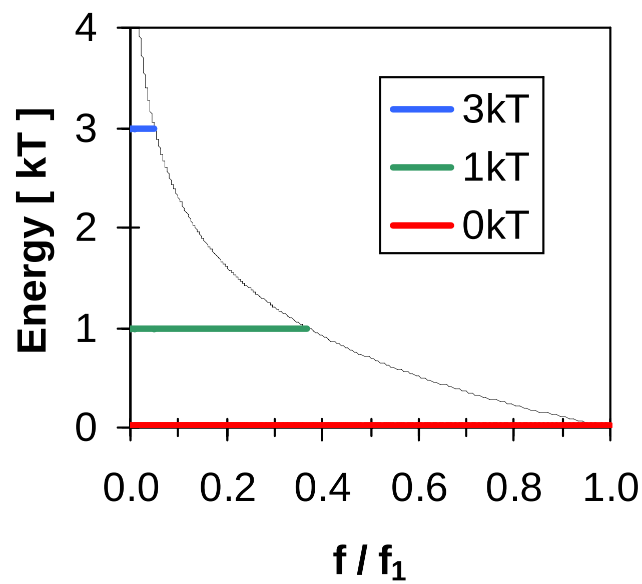

Population Mechanisms

Stimulated processes:
- **Ground-state absorption**
- **Excited-state absorption**
- **Stimulated emission**

Spontaneous processes:
- **Luminescence decay**
- **Multiphonon relaxation**

Interionic processes:
- **Energy migration**
- **Cross-relaxation**
- **Energy-transfer upconversion**

Luminescence Decay

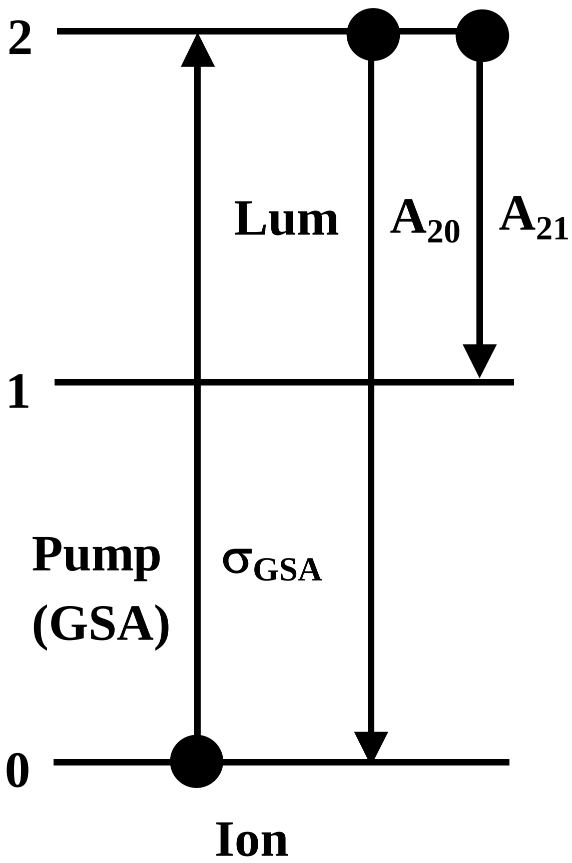

Einstein coeff. *A* for spontaneous emission

$$\sum_j A_{ij} = A_i = \tau_{i,rad}^{-1}$$ **radiative rate constant**

Lifetime

$$\tau_i^{-1} = A_i + W_i$$ **(rad. + nonrad. decay)**

Radiative rate constant,
emission cross-section,
oscillator strength
are directly connected with each other.

Decay rate: $R_{ij} = -A_{ij} N_i$

MESA+ Institute for Nanotechnology

m.pollnau@ewi.utwente.nl

Integrated Optical MicroSystems (IOMS)

University of Twente
Enschede - The Netherlands

Multiphonon Relaxation: Consequences for Lifetime

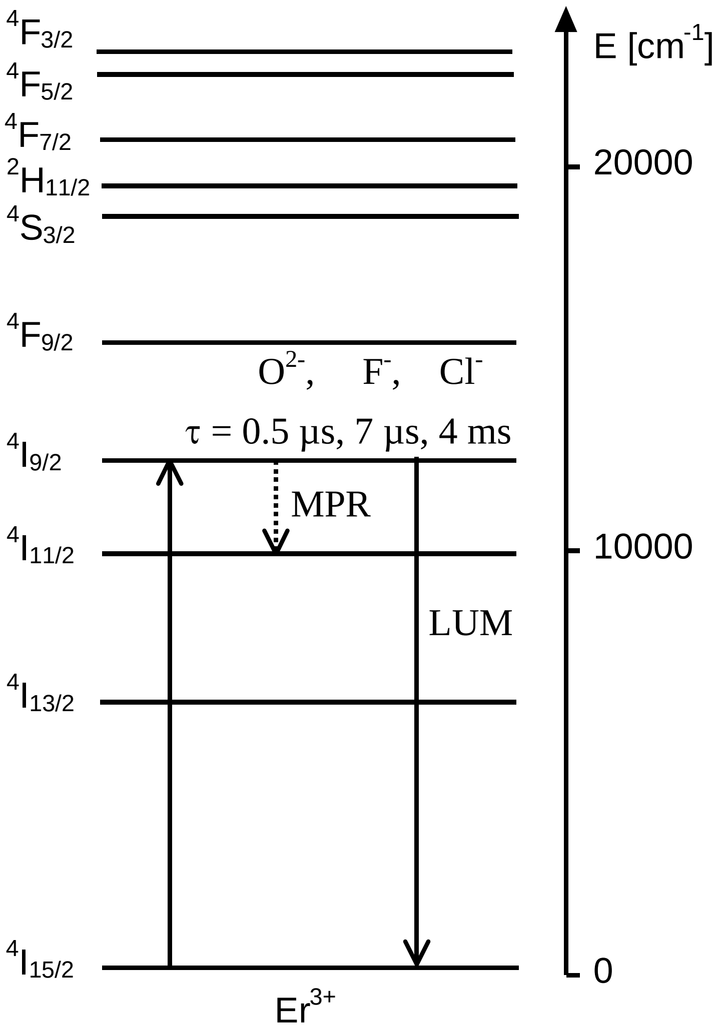

Example:

Decay from the $^4I_{9/2}$ level of Er^{3+} (to next lower-lying level: $\Delta E \approx 2000\ cm^{-1}$)

Competition between luminescence decay and multiphonon relaxation

Number of highest-energy phonons required to bridge ΔE:

Oxide: $p \approx 2 \Rightarrow \tau = 0.5\ \mu s$
Fluoride: $p \approx 4 \Rightarrow \tau = 7\ \mu s$
Chloride: $p \approx 7 \Rightarrow \tau = 4\ ms$

Upconversion Mechanisms

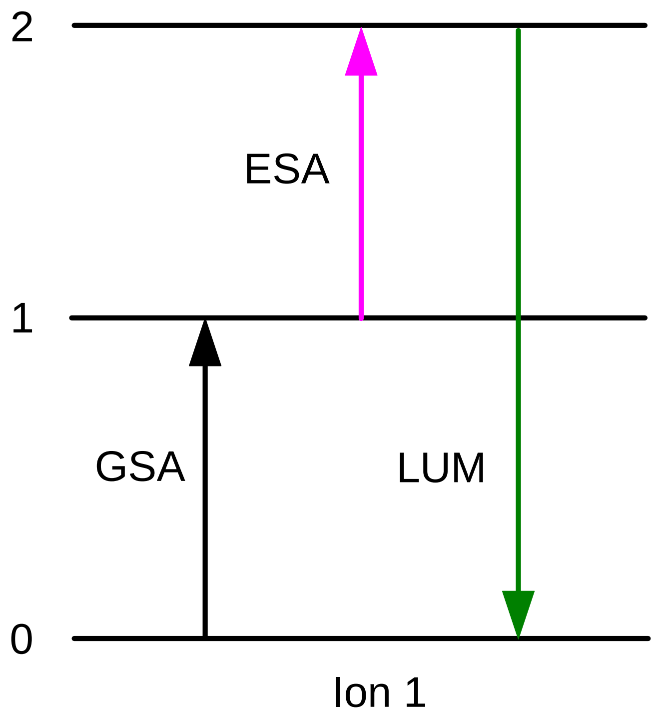

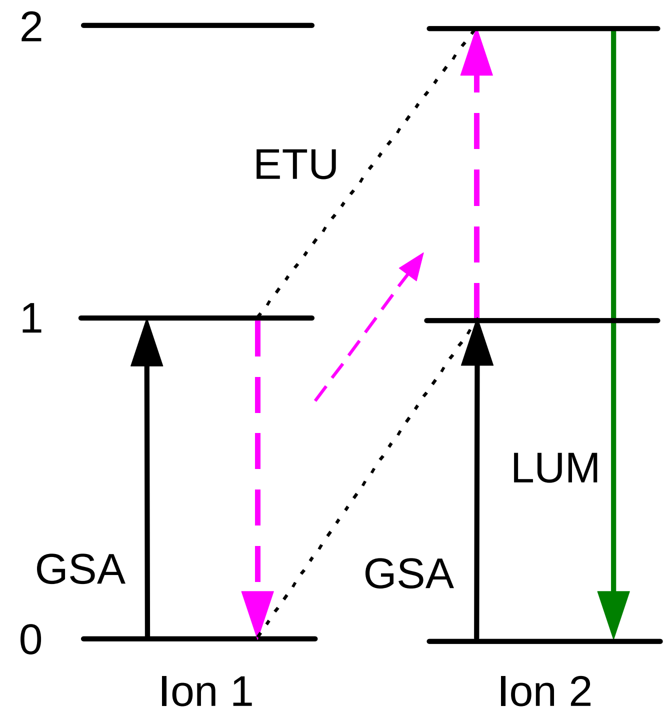

Intraionic process: ESA

(Excited-state absorption)

Interionic process: ETU

(Energy-transfer upconversion)

Energy-Transfer Processes

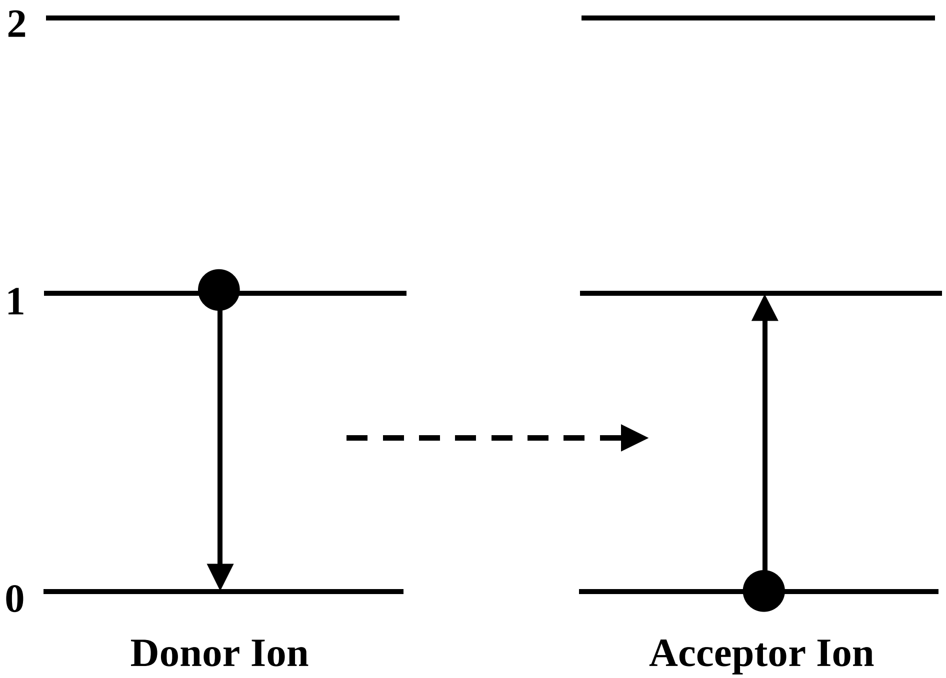

Interaction mechanisms:

1. multipole-multipole interaction:
One oscillating multipole forces another nearby multipole to oscillate as well.

2. exchange interaction:
Direct overlap between the atomic functions of two nearby ions

Most common:
Electric dipole-dipole interaction

Electric Dipole-Dipole Transfer

Transfer probability donor (*D*) $\rightarrow$ acceptor (*A*)

$$R_{DA} = \frac{3\hbar^4 c^4}{4\pi n^4} \frac{Q_A}{\tau_D} \frac{1}{r_{DA}^6} \int f_D(E) F_A(E) E^{-4} dE$$

D.L. Dexter, J. Chem. Phys. 21 (1953) 836

Q_A = integral absorption cross-section of *A*
(measure of absorption probability)
τ_D = radiative lifetime of *D*
(measure of emission probability)
f_D, F_A = normalized emission, absorption line shapes of *D*, *A*
(integral is measure of spectral overlap)
r_{DA} = distance between *D* and *A* ($R_{\mathrm{DA}} \propto r^{-6}$!!!)

Energy Migration

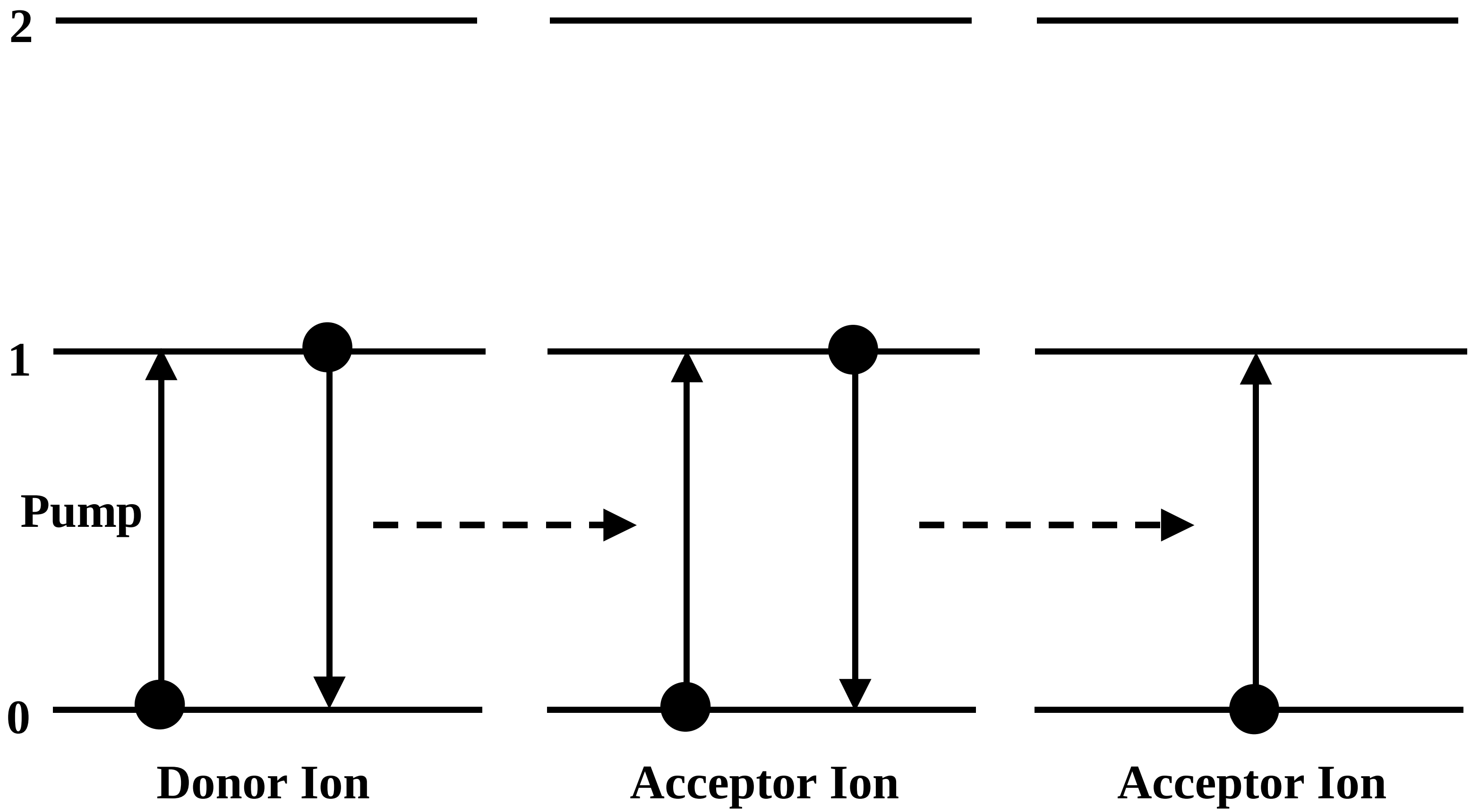

Sensitization and Quenching

Sensitization

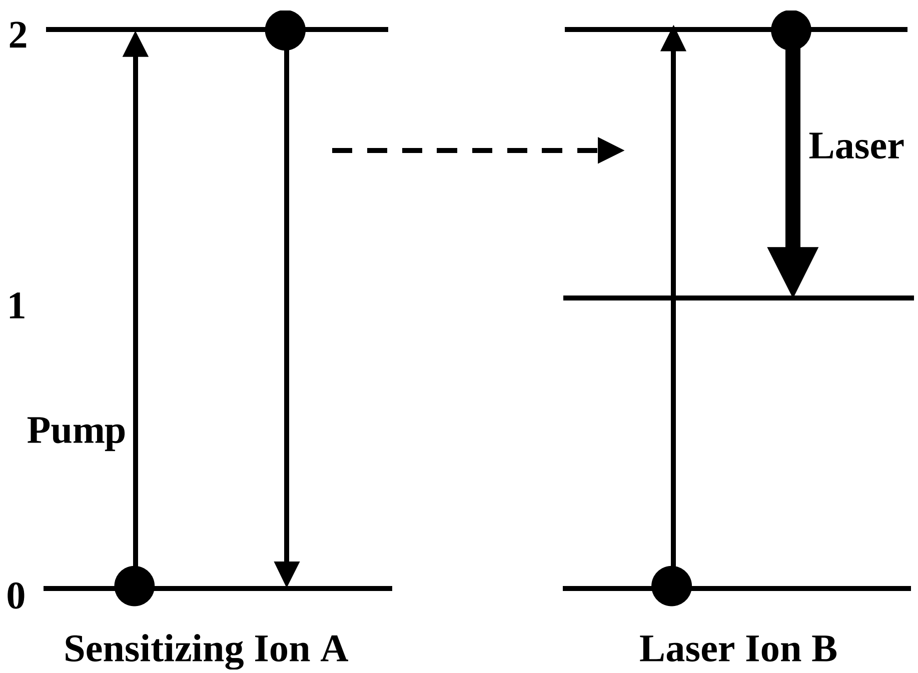

Quenching

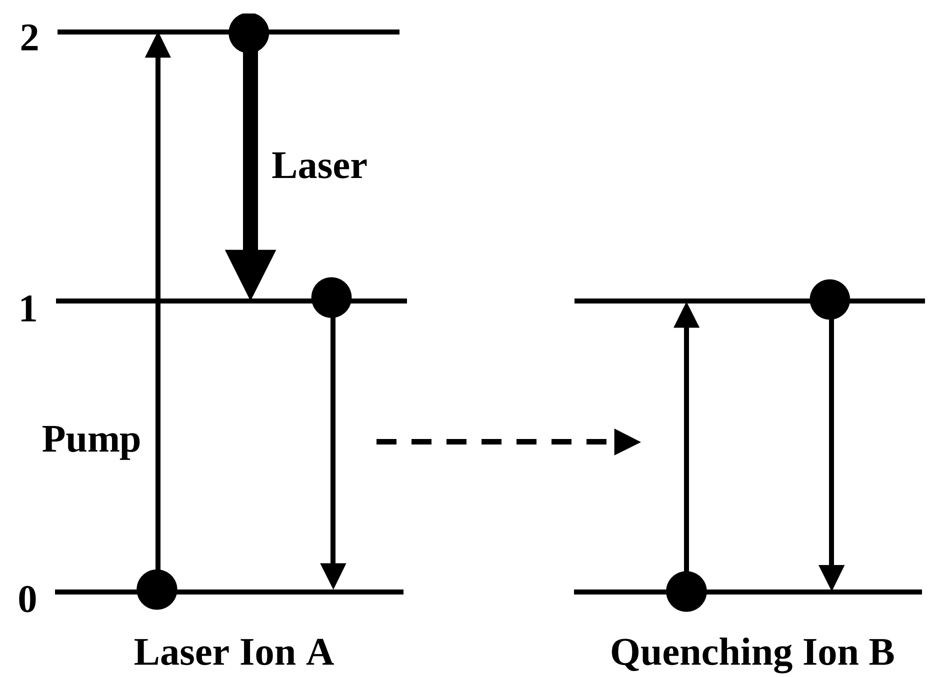

Cross-Relaxation and Energy-Transfer Upconversion

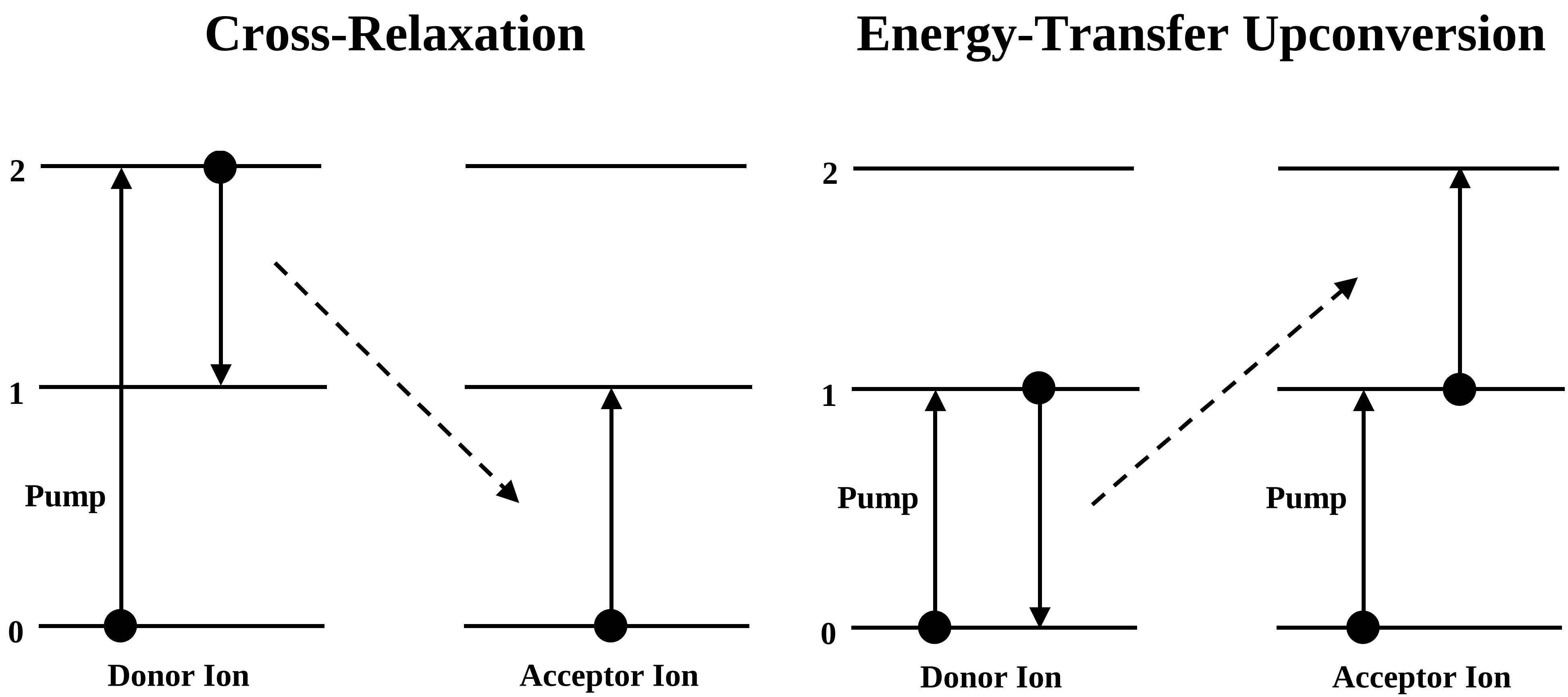

Laser Wavelengths for Micro-Surgery

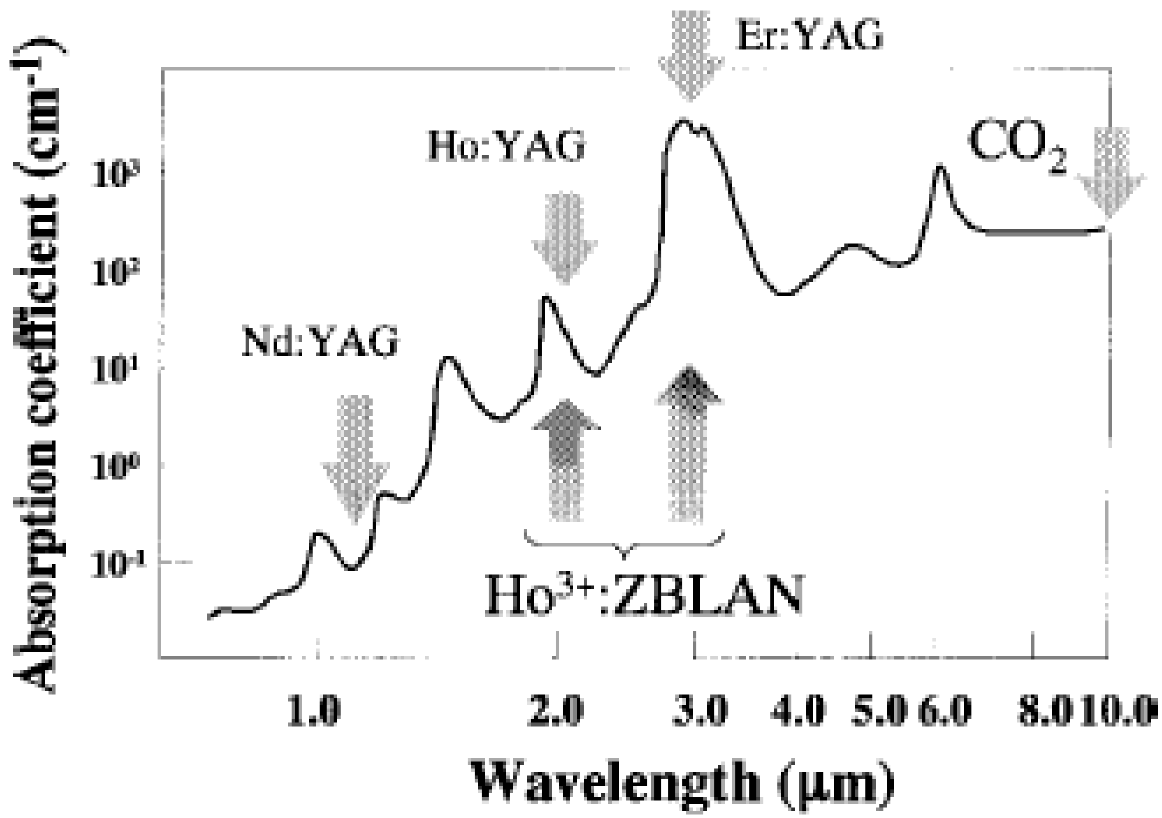

T. Sumiyoshi, IEEE J. Select. Topics Quantum Electron. 5 (1999) 936

3-µm Erbium Laser: A « simple » Four-Level Laser

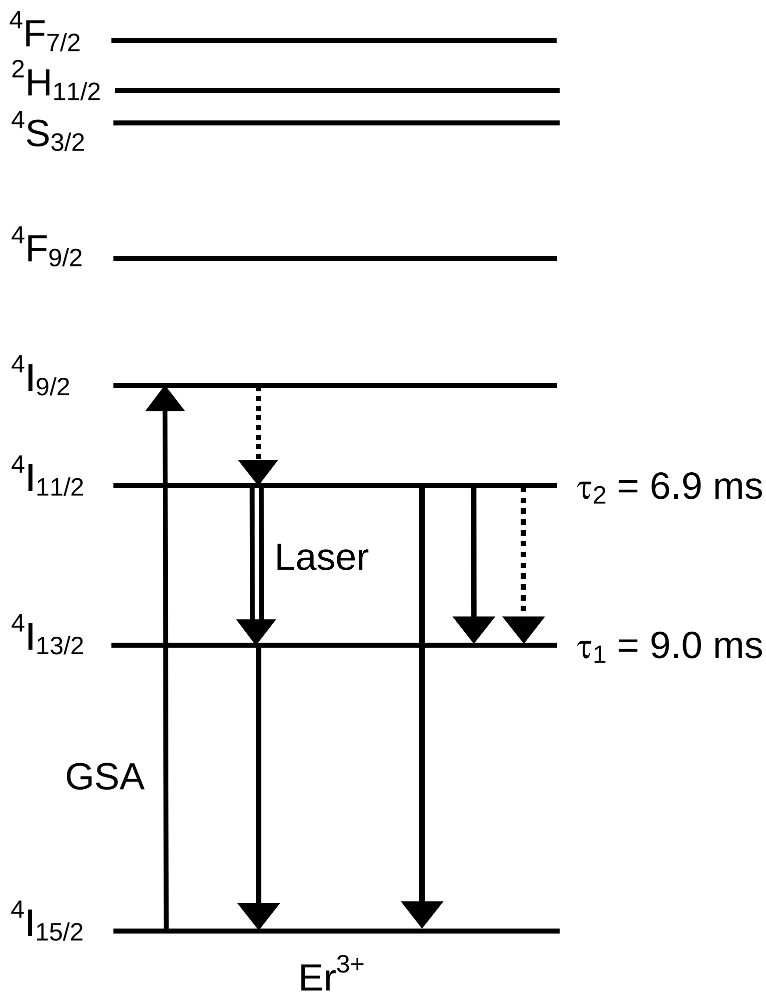

"Bottleneck" owing to longer lower level lifetime ⇒

"self-terminating" transition in continuous-wave operation.

CW inversion due to
1. **weak feeding of lower level (host materials with low maximum-phonon energy)**
2. **Stark splitting**

Depletion of lower laser level is desired to overcome bottleneck

The Erbium 3-µm Laser

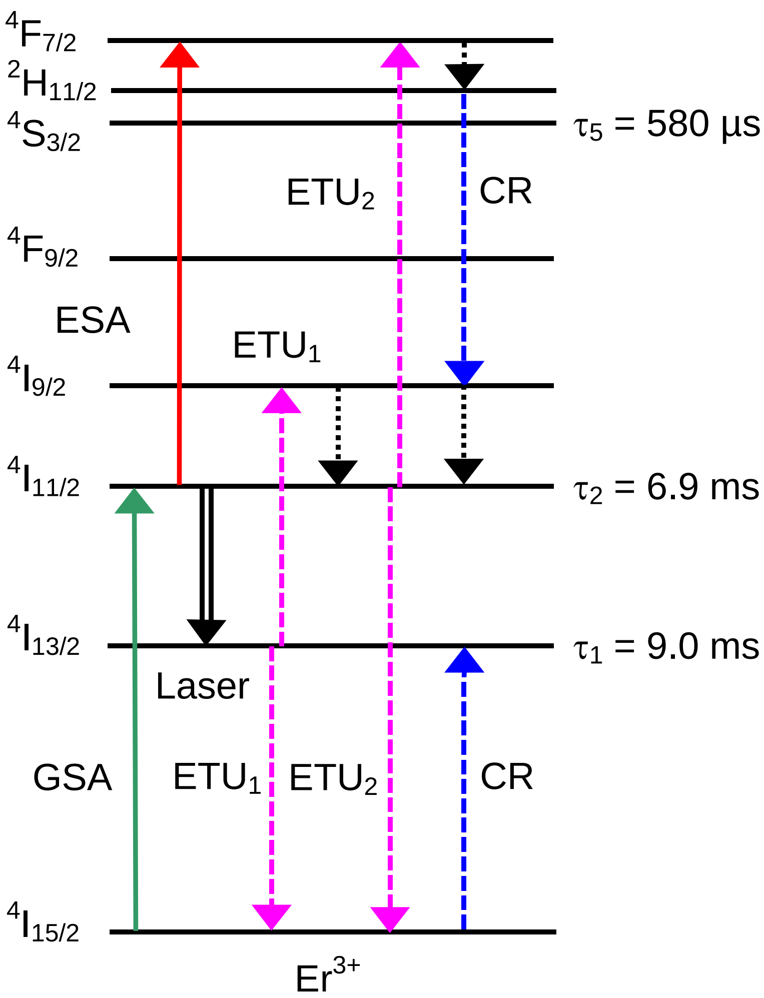

Important processes:

Pump GSA @ 800 nm or 980 nm

Pump ESA @ 800 nm or 980 nm

ETU involving two ions in lower (1) or upper (2) laser level

Cross Relexation (CR)

Depletion of Lower Laser Level

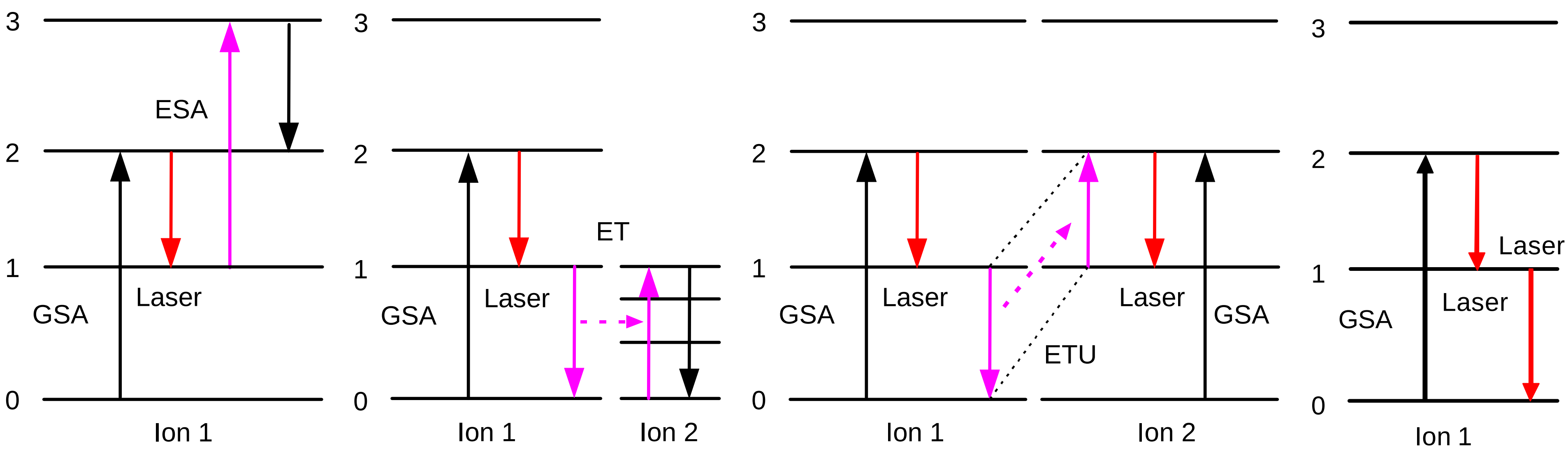

ESA **Energy Transfer** **ETU** **Laser**

ZBLAN Fiber Laser at Low Dopant Concentration

Core-pumped fiber with typically
0.1 mol. % (1000 ppm molar) (1.6×10^{19} cm^{-3})

Low dopant concentration in combination with high-intensity core pumping favors ground-state bleaching

ESA becomes stronger than GSA

ETU is not important because of large distance between ions

Excited-State Absorption

GSA = Ground-State Absorption

ESA = Excited-State Absorption

SE = Stimulated Emission

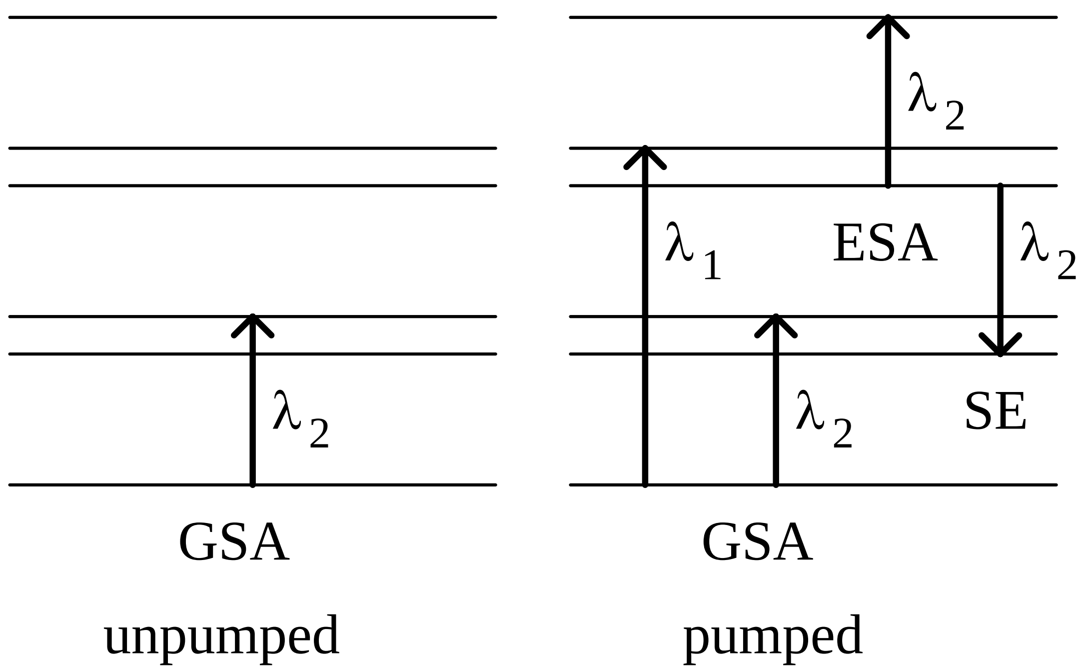

λ_1 = pump wavelength (strong laser)

λ_2 = probe wavelength (broadband lamp)

m.pollnau@ewi.utwente.nl

Integrated Optical MicroSystems (IOMS)

ESA Measurement

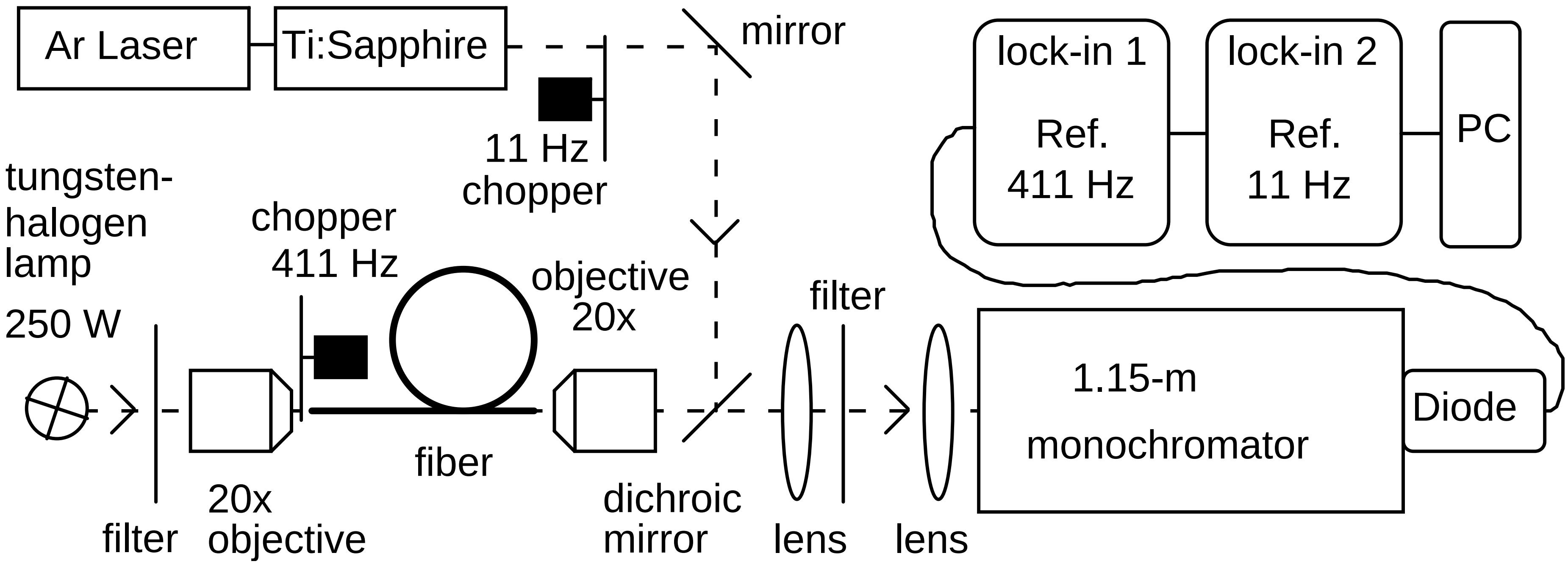

S. Zemon, SPIE Vol. 1373 (1990) 21

J. Koetke, Appl. Phys. B 61 (1995) 151

M. Pollnau, Appl. Phys. B 67 (1998) 23

Double Lock-in Amplifier Technique

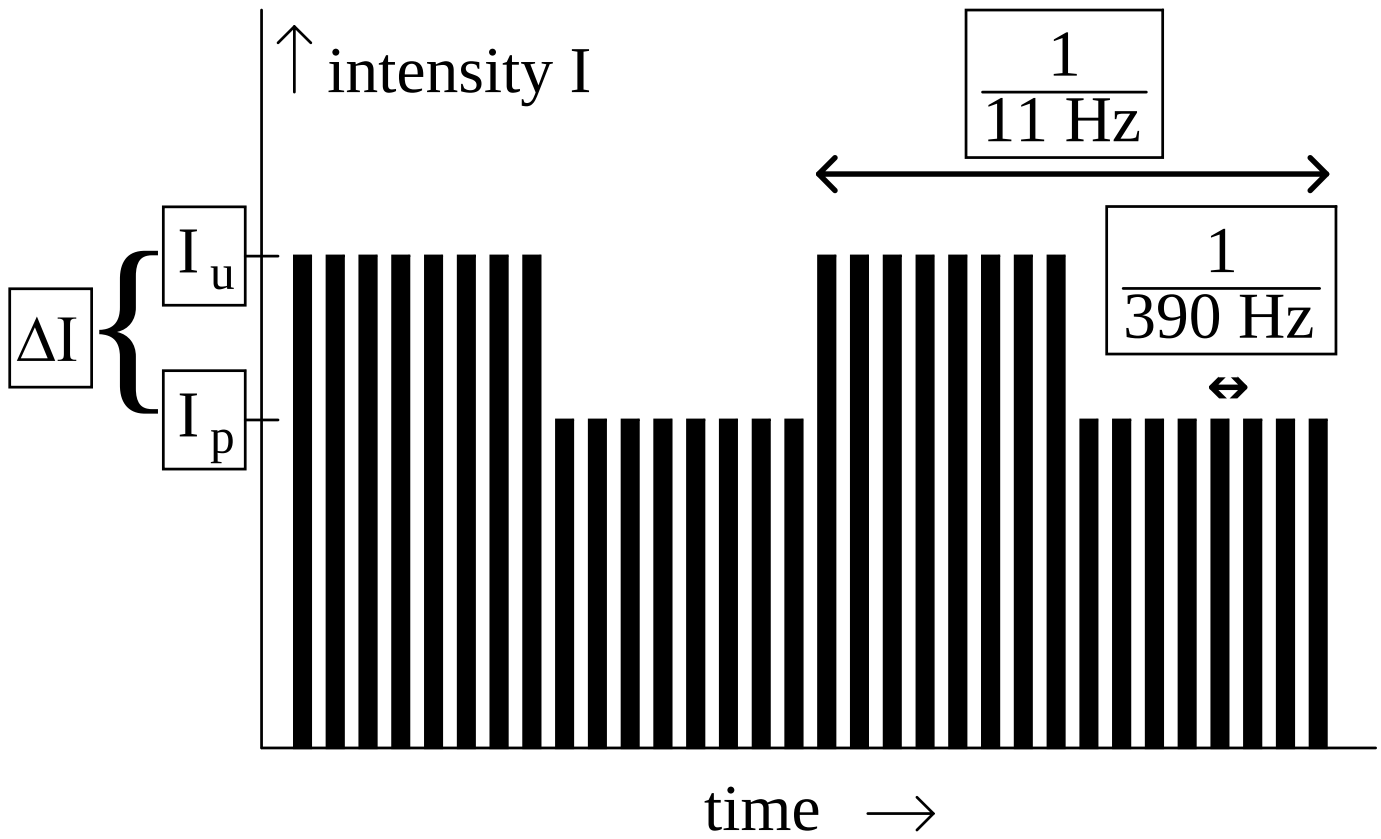

2. Lock-in:

Ref. 11 Hz ,
detects ΔI

1. Lock-in:

Ref. 390 Hz ,
detects I_u or I_p

Determination of ESA Cross-Sections

Transmitted probe-beam intensity:

unpumped:

$$I_u = I_0 \exp\left\{ -d \cdot N_e \cdot \sigma_{ESA} \right\}$$

pumped:

$$I_p = I_0 \exp\left\{ d \left[-\left(1 - N_e\right) \cdot \sigma_{GSA} - \sum_i N_i \cdot \sigma_{ESA,i} + \sum_i N_i \cdot \sigma_{SE,i} \right] \right\}$$

Calculation:

$$\frac{1}{N_e \cdot d} \ln\left(\frac{I_u}{I_p} \right) + \sigma_{GSA} = \sum_i \left[\frac{N_i}{N_e} \left(\sigma_{ESA,i} - \sigma_{SE,i} \right) \right]$$

M. Pollnau, Appl. Phys. A 54 (1992) 404

M. Pollnau, Appl. Phys. B 67 (1998) 23

Determination of ESA Cross-Sections

Measure GSA cross-section σ_{GSA}, probe-beam intensities I_u, I_p

Fit excitation density N_e until measured bleaching is completely compensated by addition of GSA (at wavelengths where no ESA or SE occurs)

Obtain ESA cross-sections $\sigma_{ESA,i}$ times relative population densities N_i/N_e

Determine relative population densities N_i/N_e and calculate ESA cross-sections $\sigma_{ESA,i}$

M. Pollnau, Appl. Phys. A 54 (1992) 404

M. Pollnau, Appl. Phys. B 67 (1998) 23

ESA at 800 nm in ZBLAN:Er^{3+}

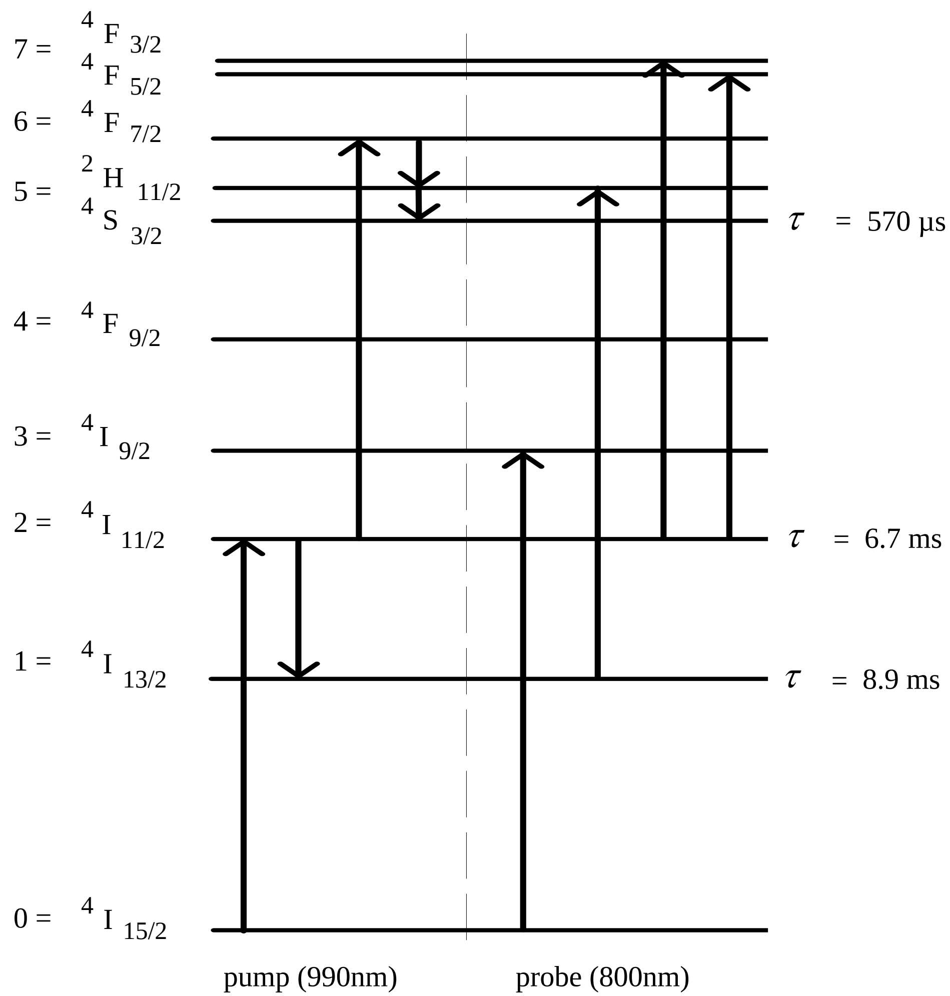

m.pollnau@ewi.utwente.nl

Integrated Optical MicroSystems (IOMS)

ESA Cross-Sections Near 800 nm

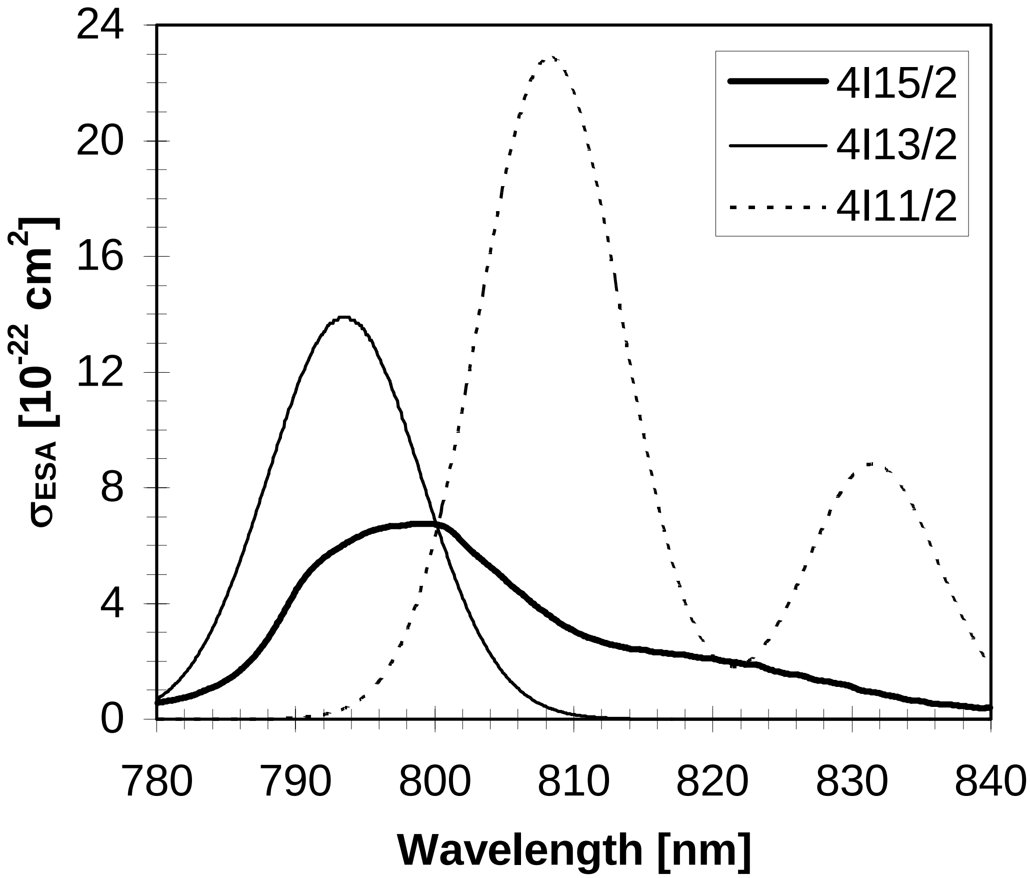

ESA cross sections determined from pump- and probe-beam measurements

M. Pollnau, Appl. Phys. B 67 (1998) 23

Best pump wavelength at 792 nm:

Relatively strong GSA,

Strong ESA from $^4I_{13/2}$,

Weak ESA from $^4I_{11/2}$

The Cascade-Lasing Regime

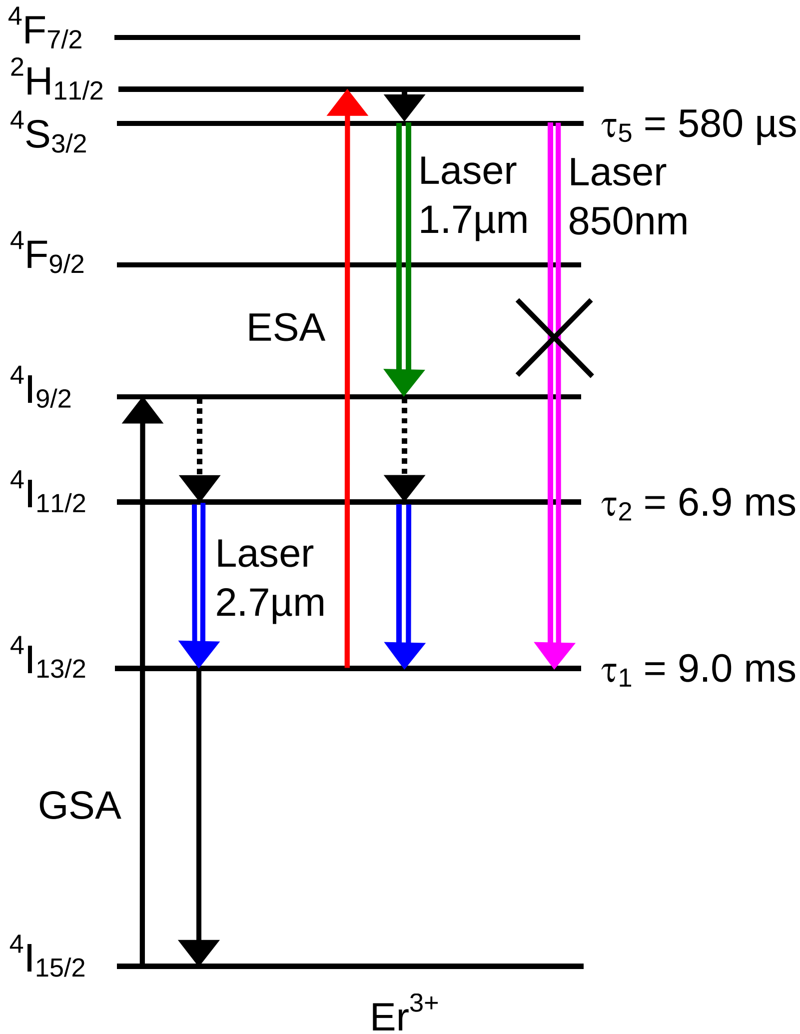

Two-loop cascade laser:

ESA depletes lower laser level of 2.7-µm laser

$^4S_{3/2}$ level clamped to threshold inversion by 1.7-µm laser, energy recycled

Competitive 850-nm laser $^4S_{3/2} \rightarrow {}^4I_{13/2}$ (bypasses upper and populates lower laser level) is suppressed

Performance Under Cascade Lasing

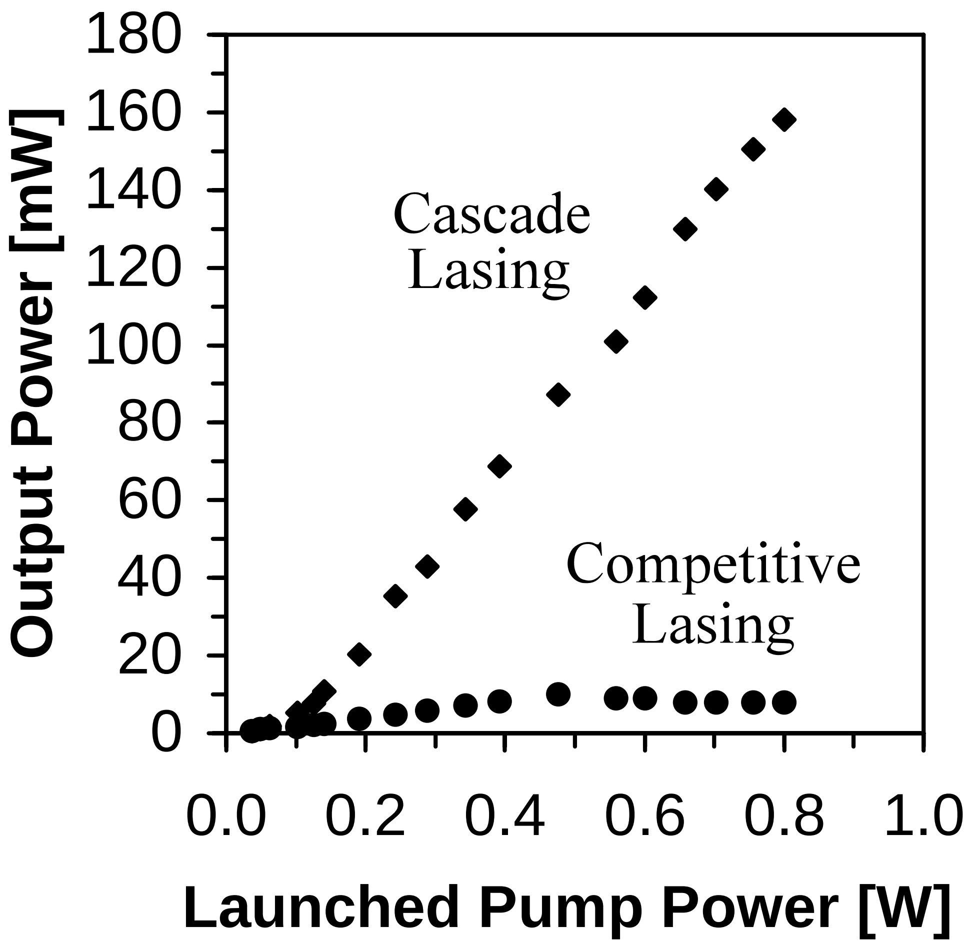

Ti:sapphire core-pumped ZBLAN fiber laser at 2.7 µm:

Strong increase of slope eff. and output power at the onset of cascade-lasing:

Slope eff. 23%

Output power 150 mW

M. Pollnau, Appl. Phys. Lett. 66 (1995) 3564

ZBLAN Fiber Laser at Medium Dopant Concentration

Cladding-pumped fiber with typically
1 mol. % (10000 ppm molar) (1.6×10^{20} cm^{-3})
co-doped with Pr^{3+}

Higher dopant concentration in combination with low-intensity cladding pumping and lifetime quenching by Pr^{3+} favors ET

Ground-state bleaching and ESA are not important because of higher dopant concentration and low pump intensity

Er^{3+} Lifetimes in the Presence of Pr^{3+}

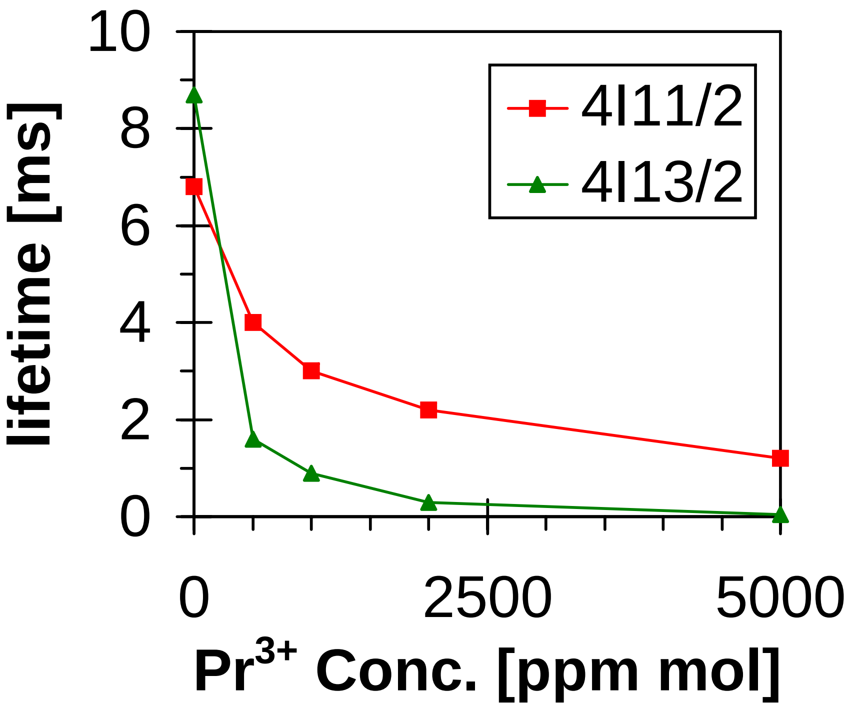

Lifetimes of $^4I_{11/2}$ upper and $^4I_{13/2}$ lower laser levels vs. Pr^{3+} concentration

Quenching of lower level lifetime much stronger (from 9 ms down to 20 µs), because corresponding absorption transition in Pr^{3+} has high oscillator strength

P.S. Golding, Phys. Rev. B 62 (2000) 856

The Lifetime-Quenching Regime

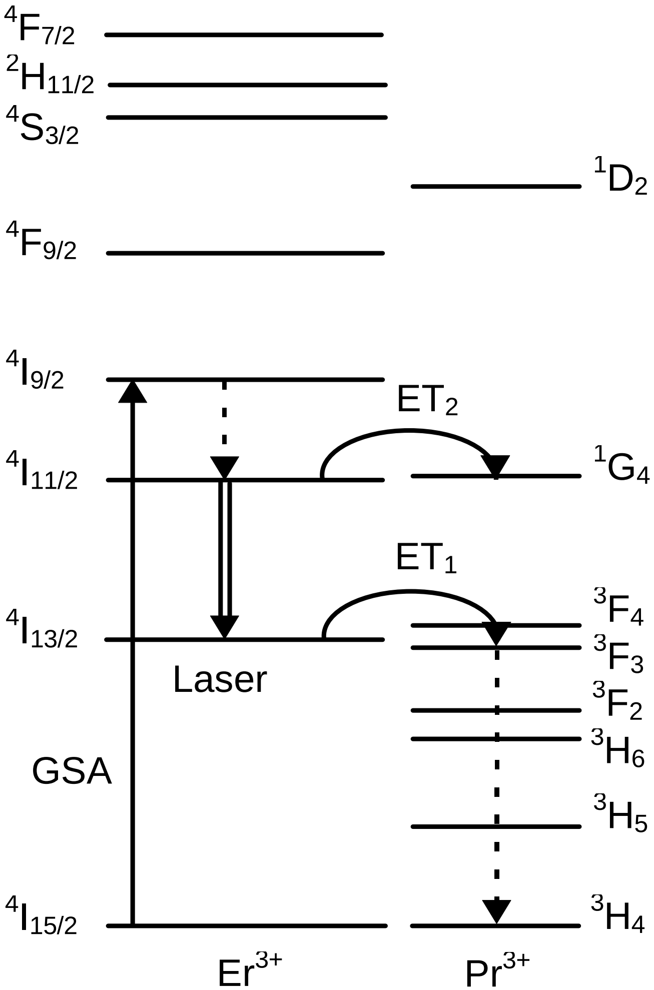

Simple four-level laser:

Energy transfer to Pr^{3+} co-dopant depletes lower laser level efficiently

CW threshold condition removes energy from $^4I_{11/2}$ upper laser level

ESA is avoided

M. Pollnau, IEEE JQE 33 (1997) 1982

Performance Under Lifetime Quenching

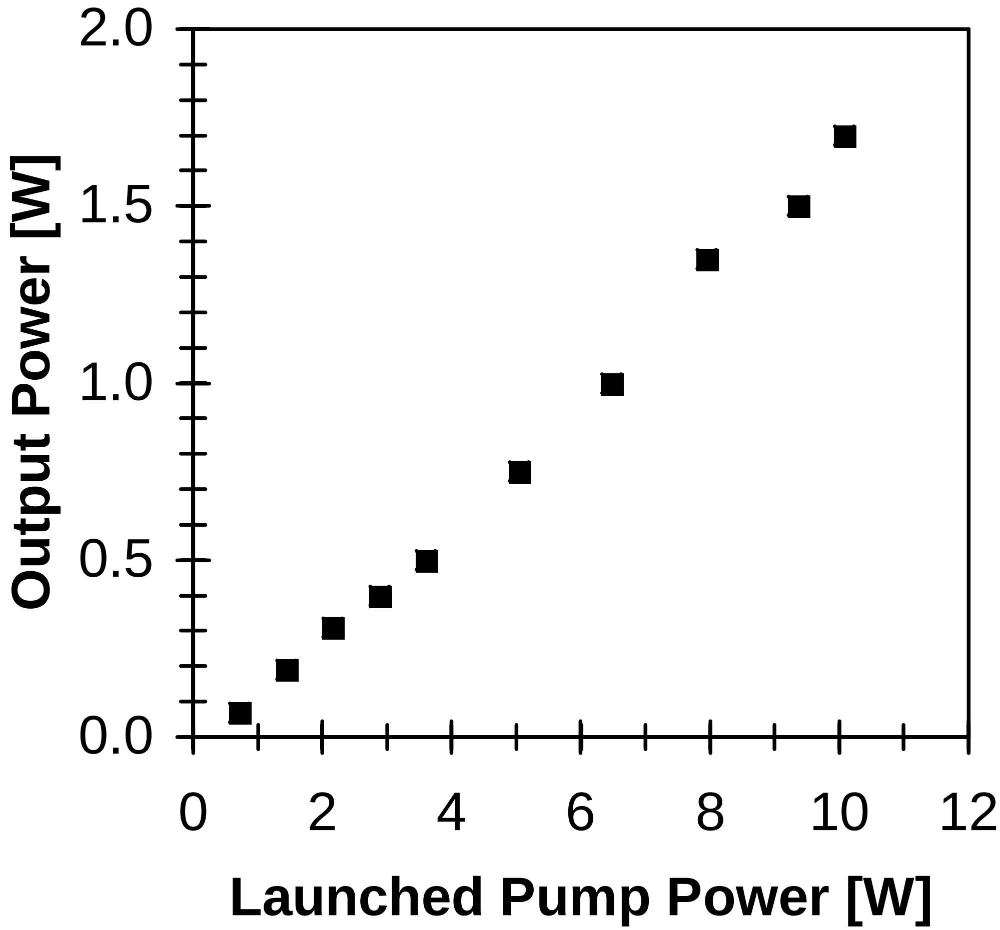

Diode-pumped double-clad ZBLAN fiber laser at 2.7 µm:

Low-brightness pump is converted to single-mode output

Slope eff. 17%

Output power 1.7 W

S. D. Jackson, Opt. Lett. 24 (1999) 1133

ZBLAN Fiber Laser at High Dopant Concentration

Cladding-pumped fiber with up to
10 mol. % (100000 ppm molar) (1.6×10^{21} cm^{-3})

High dopant concentration favors ETU

Ground-state bleaching and ESA are not important because of high dopant concentration and low pump intensity

Measurement of ETU

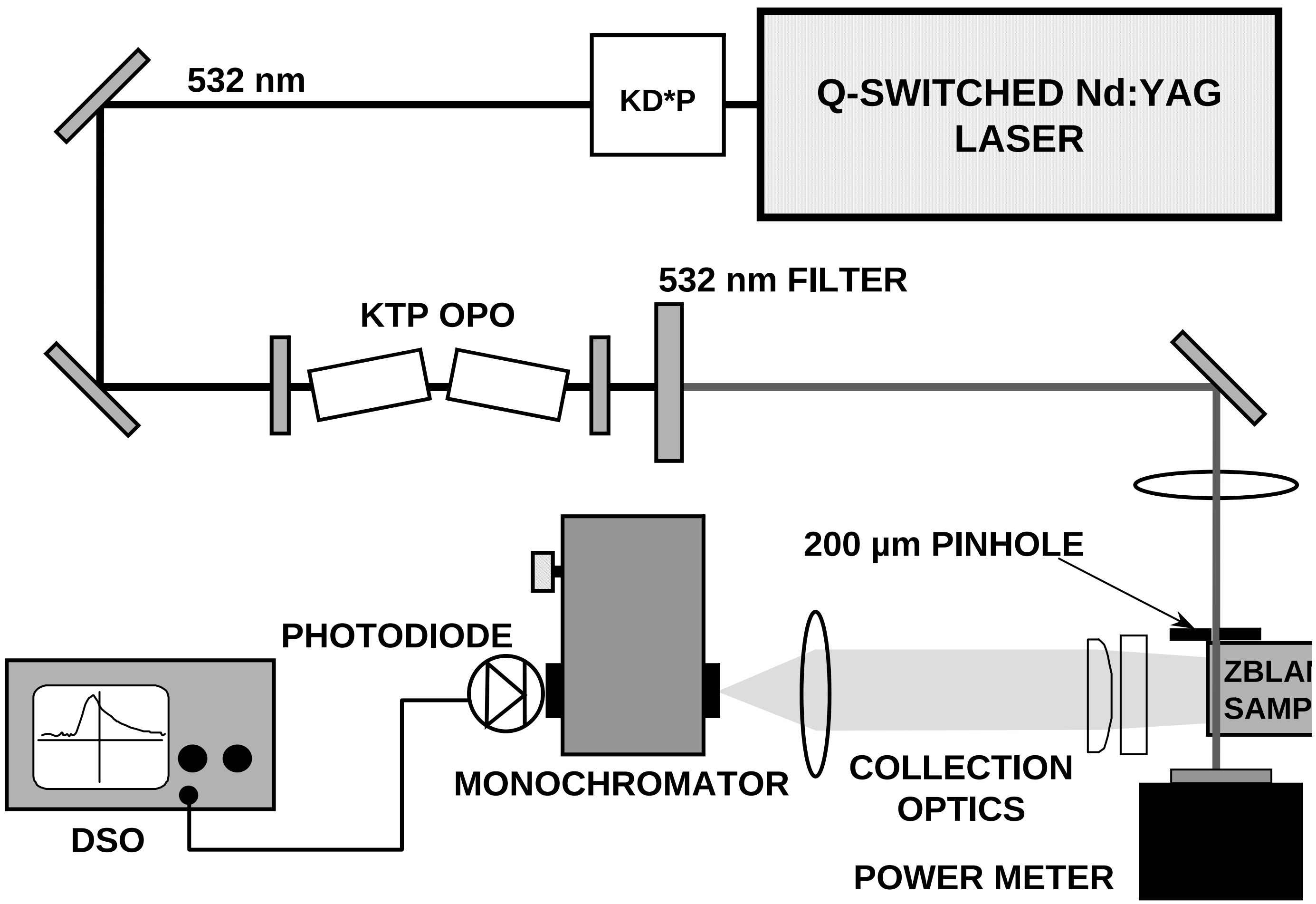

Measured Luminescence Decay

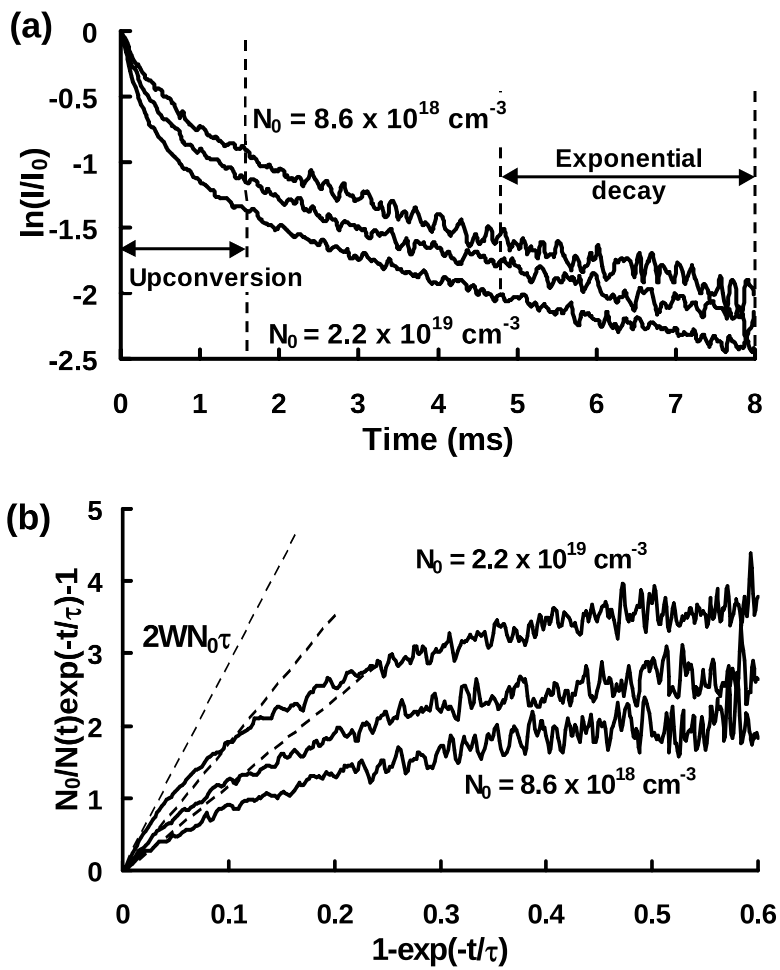

Normalized decay curves:

First temporal part:

- **high excitation density,**
- **includes decay by ETU,**
- **non-exponential**

Last temporal part:

- **low excitation density,**
- **includes no ETU,**
- **exponential**

P.S. Golding,
Phys. Rev. B 62 (2000) 856

Luminescence Decay Curves

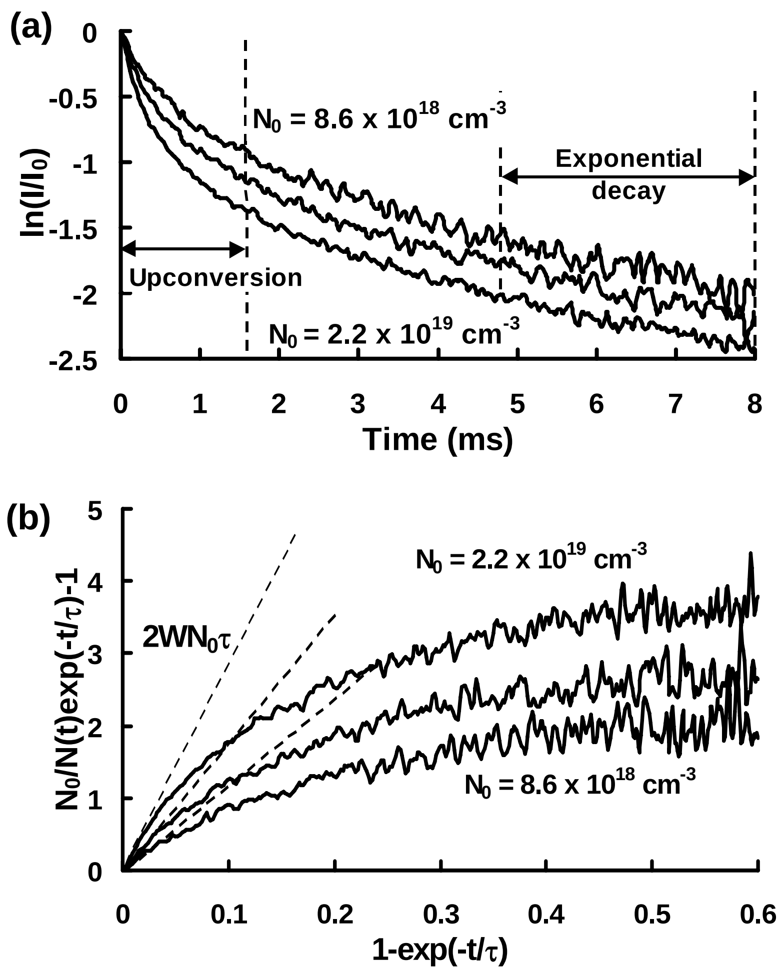

Rate-equation for decay:

$$dN/dt = -\tau^{-1} N - 2WN^2$$

Solution (Bernoulli-Eq.):

$$N(t) = \frac{N_0 \exp(-t/\tau)}{1 + 2WN_0\tau\left[1 - \exp(-t/\tau)\right]}$$

Linearized solution:

$$\left[N_0 / N(t)\right]\exp(-t/\tau) - 1 = 2WN_0\tau\left[1 - \exp(-t/\tau)\right]$$

$$Y = A \cdot X$$

T. Jensen, Ph.D. Thesis, Univ. Hamburg (2000)

Determination of ETU Parameters

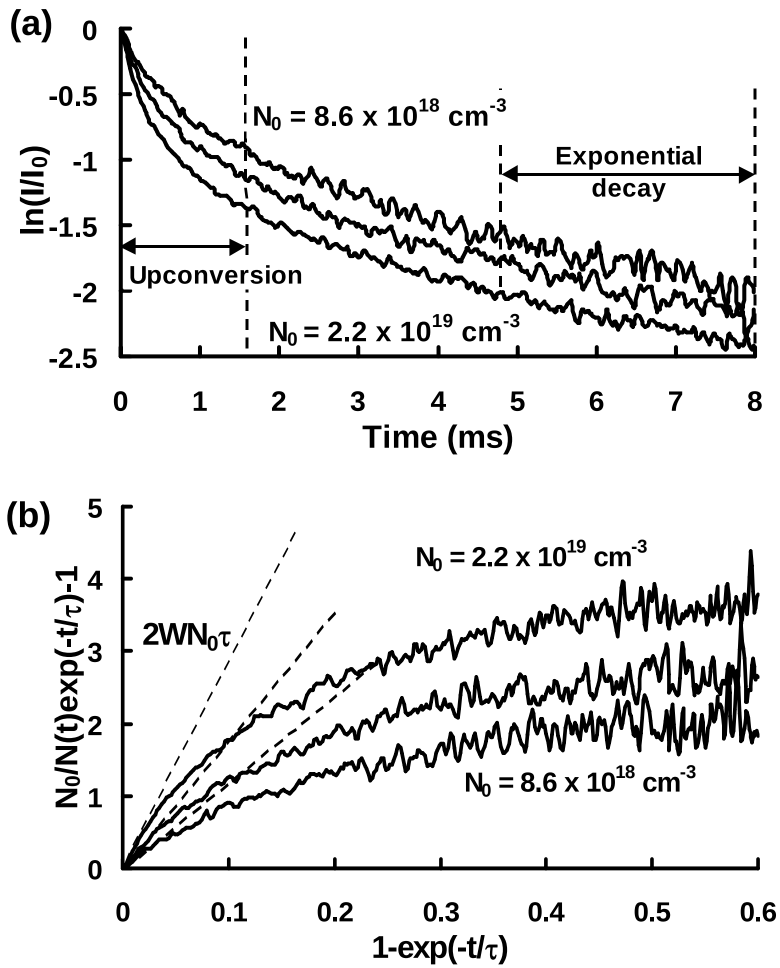

Linearized solution:

$$\left[N_0 / N(t)\right]\exp(-t/\tau)-1$$
$$= 2WN_0\tau\left[1-\exp(-t/\tau)\right]$$

Determine

t from exponential part,

N0 from excited volume and absorbed pump energy,

Fit straight lines ⇒ W

T. Jensen, Ph.D. Thesis, Univ. Hamburg (2000)

Advantage of Procedure

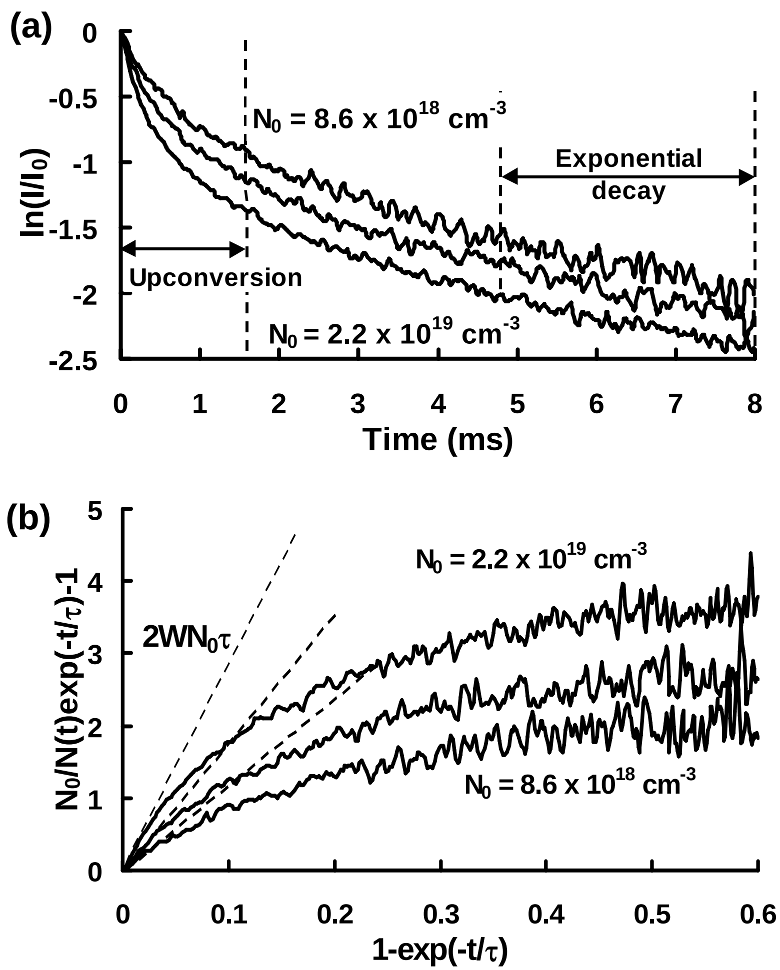

If equation were not linearized, onset of repopulation from higher levels would not be seen

⇒ complete set of rate equations from all levels must be solved

⇒ one has to know all parameters (further ETU parameters !!!)

T. Jensen, Ph.D. Thesis, Univ. Hamburg (2000)

ETU and CR Processes

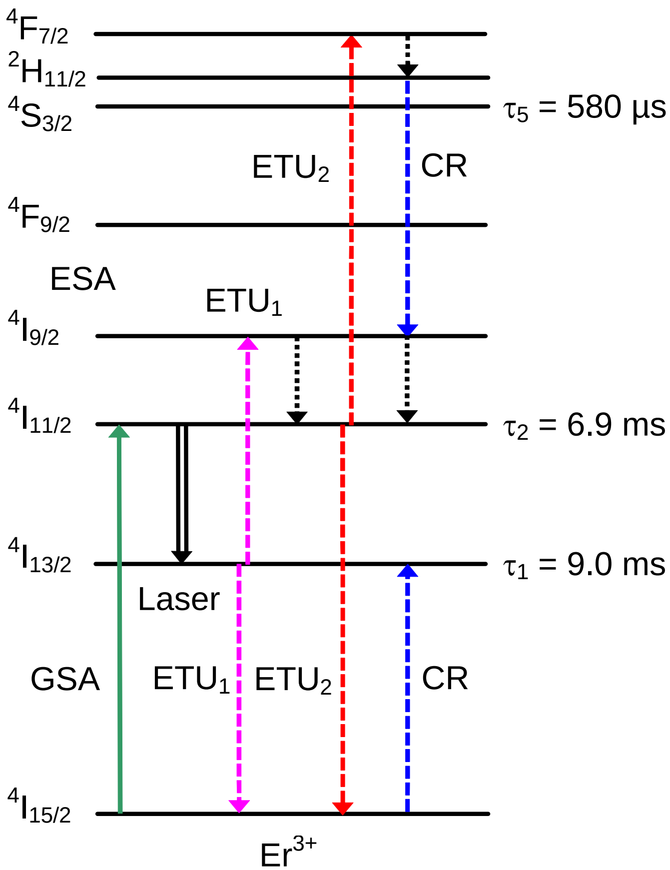

Measured parameters:

CR from $^4S_{3/2}$ level

ETU from $^4I_{11/2}$ upper laser level

ETU from $^4I_{13/2}$ lower laser level

ETU Parameters

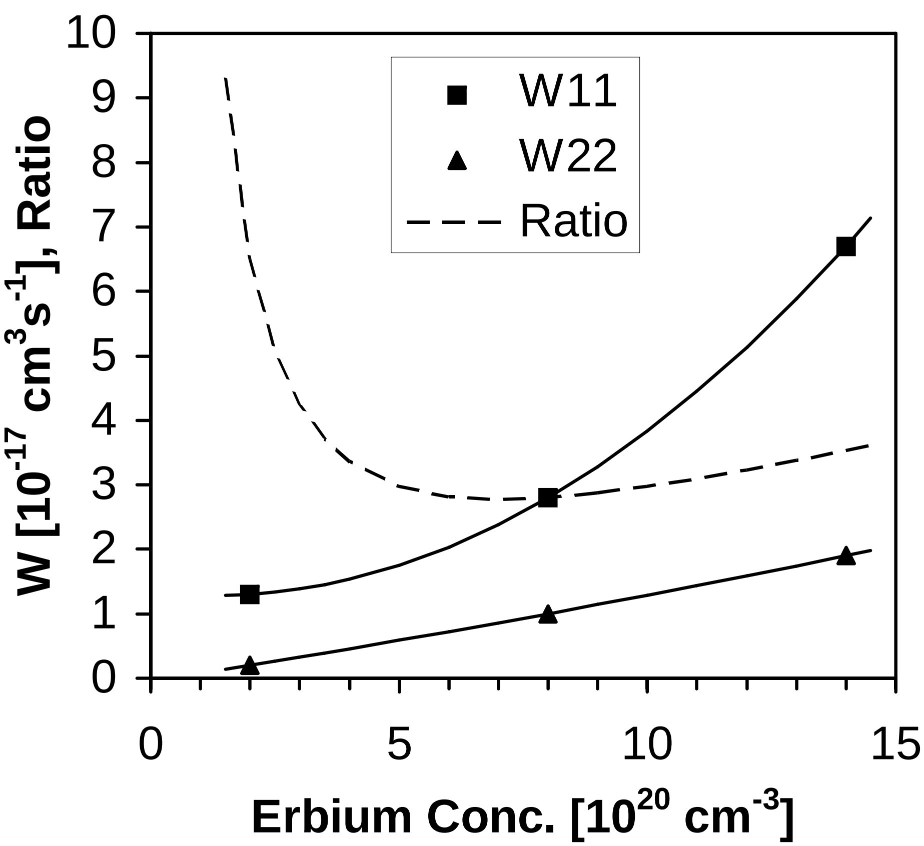

ETU parameters determined from fluorescence decay

P.S. Golding, Phys. Rev. B 62 (2000) 856

Quantum efficiency:

$$\eta_q = 2 - \frac{b_1^2}{b_2^2}\frac{W_{22}}{W_{11}}$$

Important: Ratio W_{11}/W_{22}

M. Pollnau, IEEE JQE 32 (1996) 657

The Energy-Recycling Regime

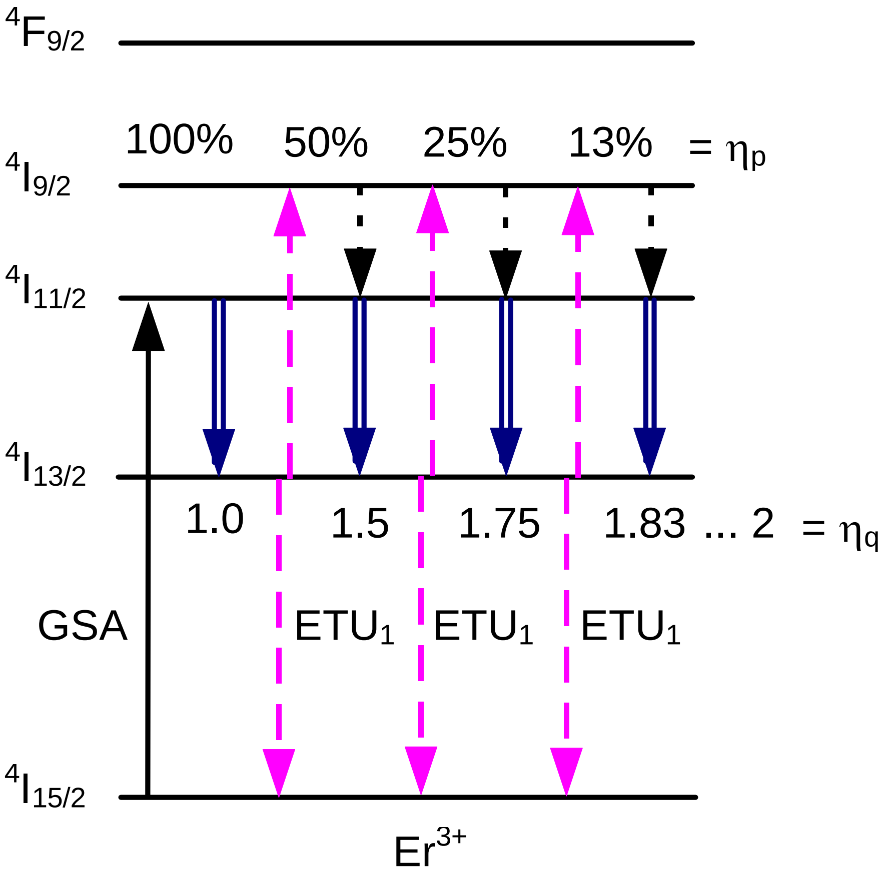

ETU processes from lower laser level ($^4I_{13/2}$) recycles energy to upper laser level ($^4I_{11/2}$)

⇒ quantum efficiency of 2

⇒ increase in slope efficiency by factor of 2

M. Pollnau, IEEE J. Select. Topics Quantum Electron. 7 (2001) 30

MESA+ Institute for Nanotechnology

m.pollnau@ewi.utwente.nl

Integrated Optical MicroSystems (IOMS)

University of Twente Enschede - The Netherlands

Comparison: Thulium 2-μm vs. Erbium 3-μm Lasers

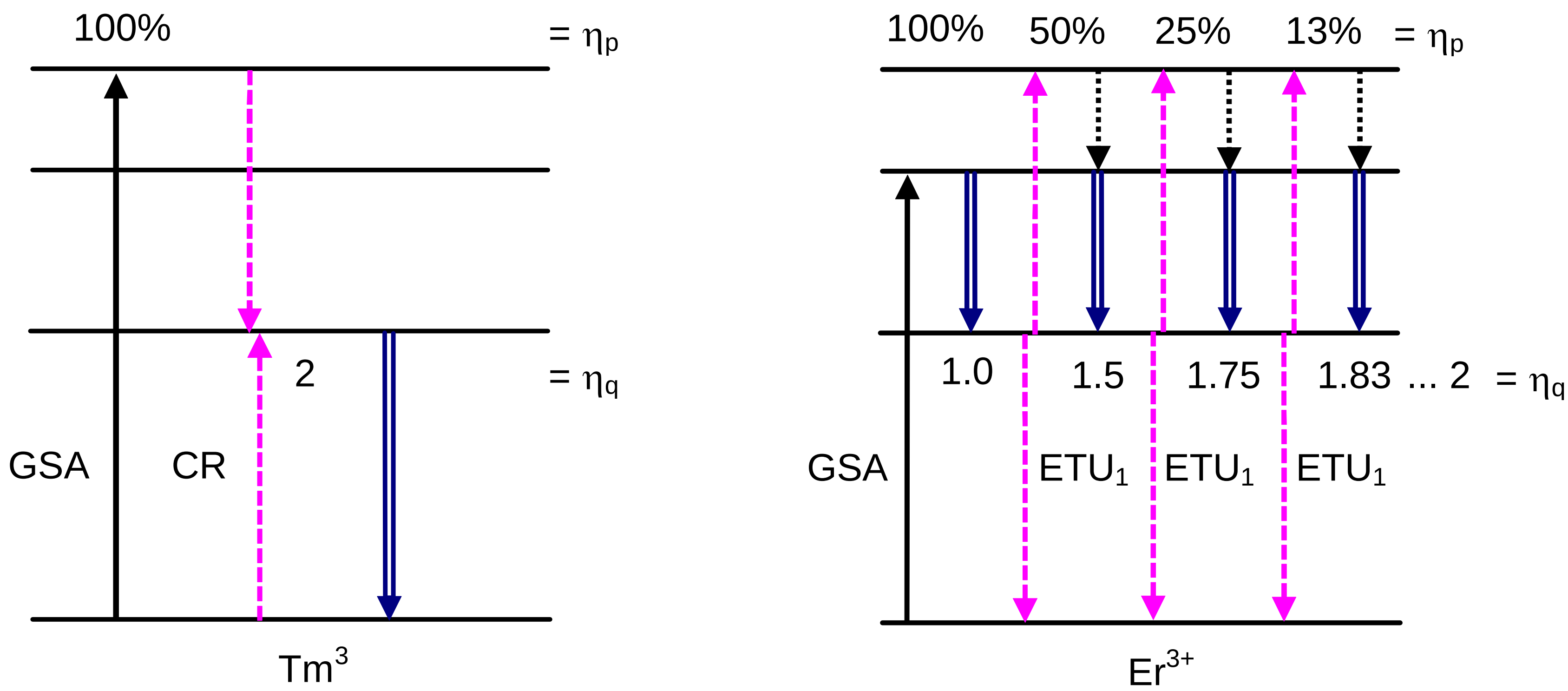

In both cases: increase in slope efficiency by factor of 2

Experimental Results in Cyrstals

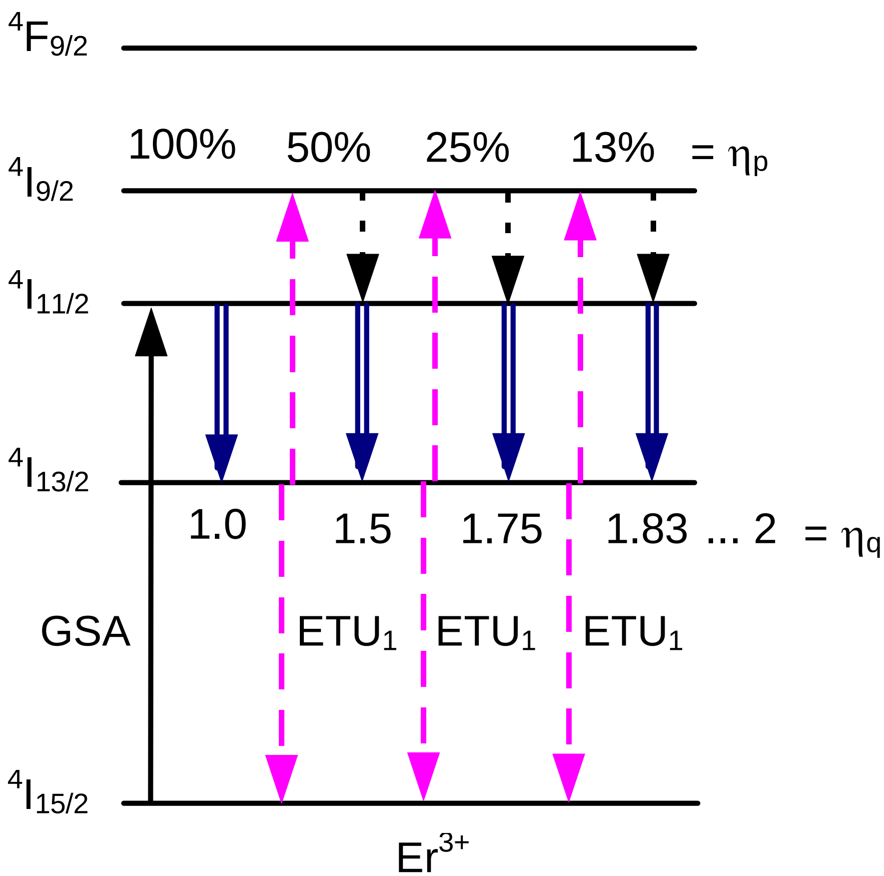

Various host materials (YLF, YAG, YSGG, GGG, ...)

~1 W output power

T. Jensen, Opt. Lett. 21 (1996) 585

~50% slope efficiency

C. Wyss, Opt. Commun. 139 (1997) 215

~2-4 W output power

A.Y. Dergachev, CLEO Technical Digest (2000), 564

Expected Fiber Performance Under Energy Recycling

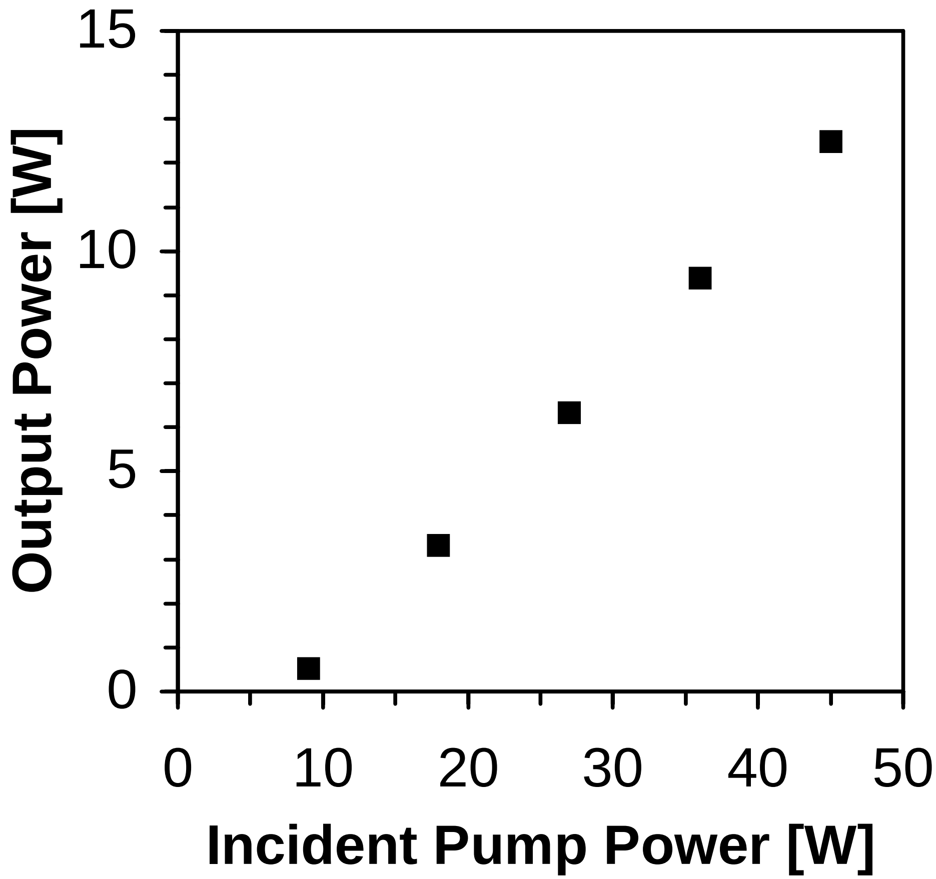

Diode-pumped double-clad ZBLAN fiber laser at 2.7 µm:

Rate-equation calculation:

ETU can be exploited

Prediction:

Slope eff. 50%

Output power >10 W

M. Pollnau, IEEE JQE 38 (2002) 162

The Thermal Problem

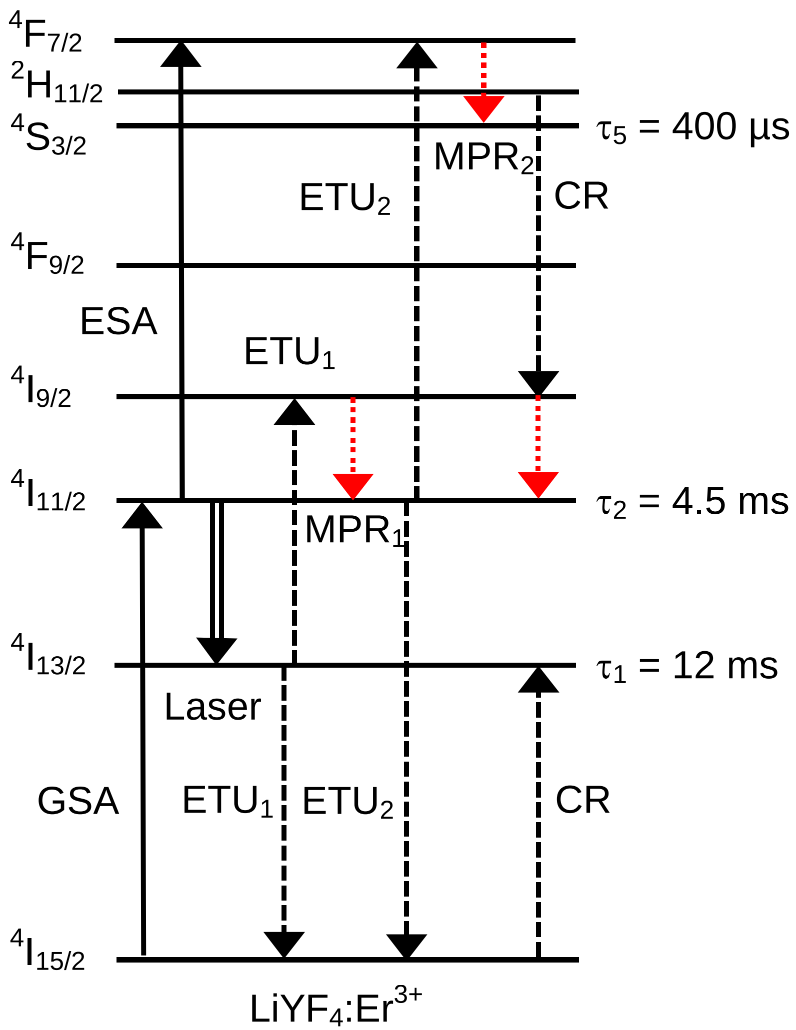

Strong heat load owing to multiphonon relaxations following the ETU processes

⇒ strong temperature increase

⇒ strong thermal lensing (crystal laser: 2x that of 1-µm Nd3+ laser!)

⇒ rod fracture

⇒ fiber melting

Example: $LiYF_4:Er^{3+}$

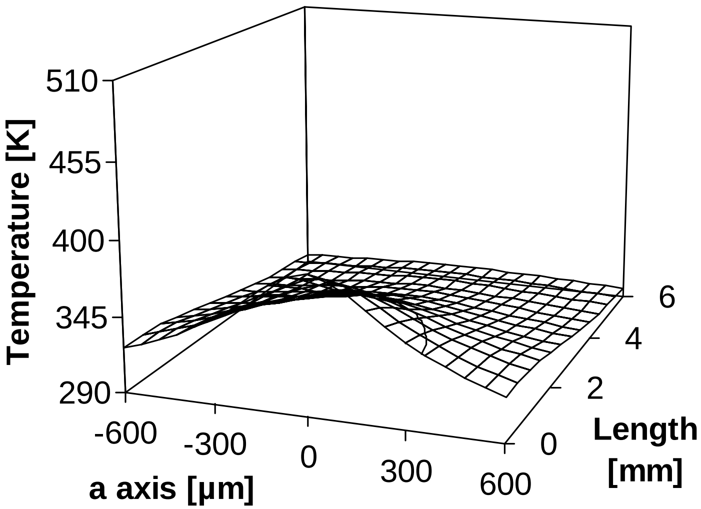

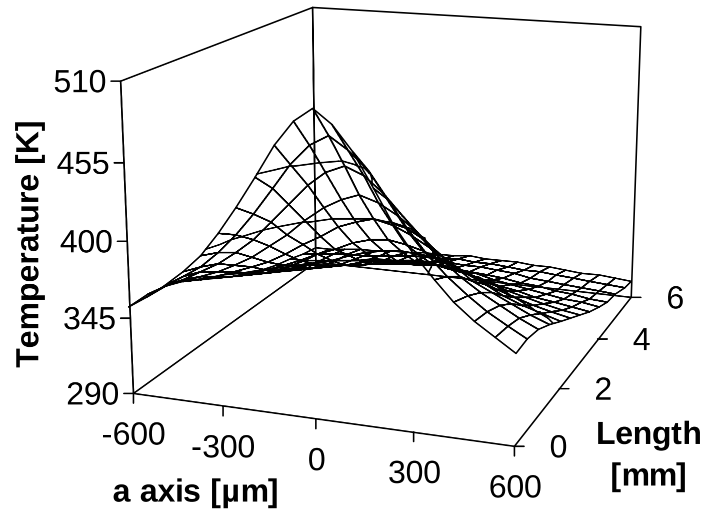

Lasing conditions **Non-lasing conditions**

M. Pollnau, IEEE J Q-E 39 (2003) 350

ZBLAN Fiber Laser at Medium Dopant Concentration

Cladding-pumped fiber with typically
0.5 mol. % (5000 ppm molar) (8×10^{19} cm^{-3})

Lower dopant concentration in combination with low-intensity cladding pumping and cascade lasing at 1.6 μm diminishes other spectroscopic processes

ESA and ETU are not that important because of low excitation density, ET is impossible because of lack of Pr^{3+}

Population Dynamics in Lower Cascade Lasing

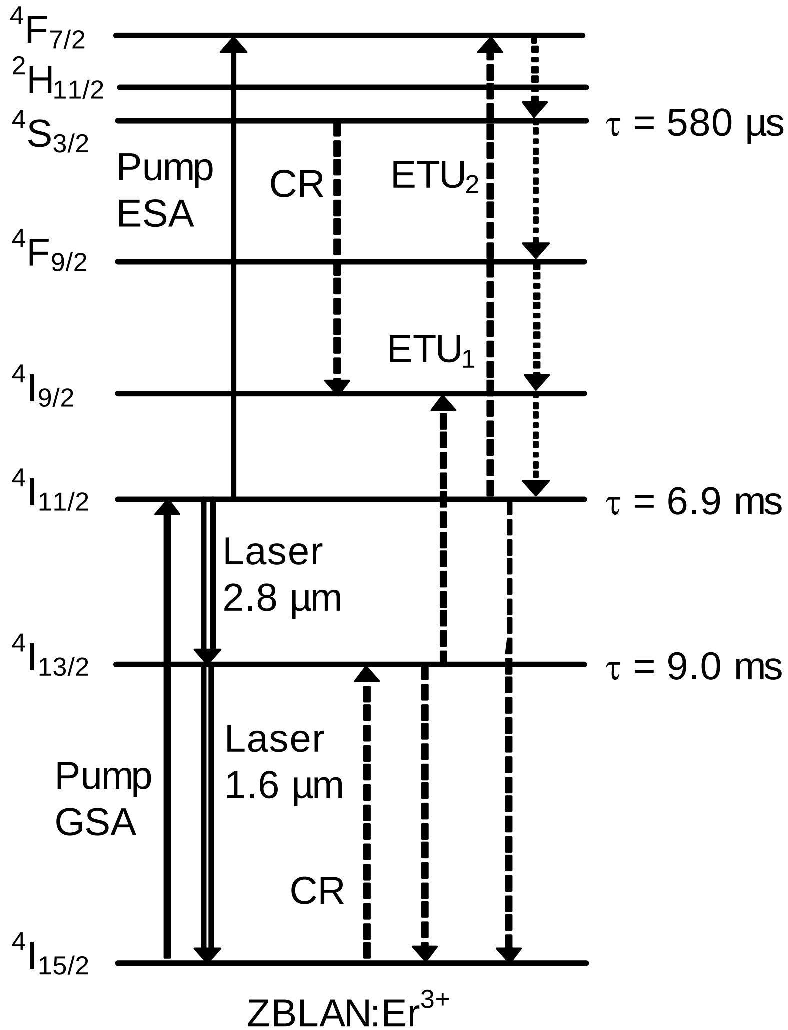

The laser at 2.8 µm starts lasing first. As soon as the laser transition at 1.6 µm reaches threshold,

$^4I_{11/2}$ is clamped to threshold inversion vs. $^4I_{13/2}$,

$^4I_{13/2}$ is clamped to threshold inversion vs. $^4I_{15/2}$.

$\Rightarrow$ All three levels remain at constant density, heat input is minimal, no parasitic processes become important.

Input-Output Curves

Experimental

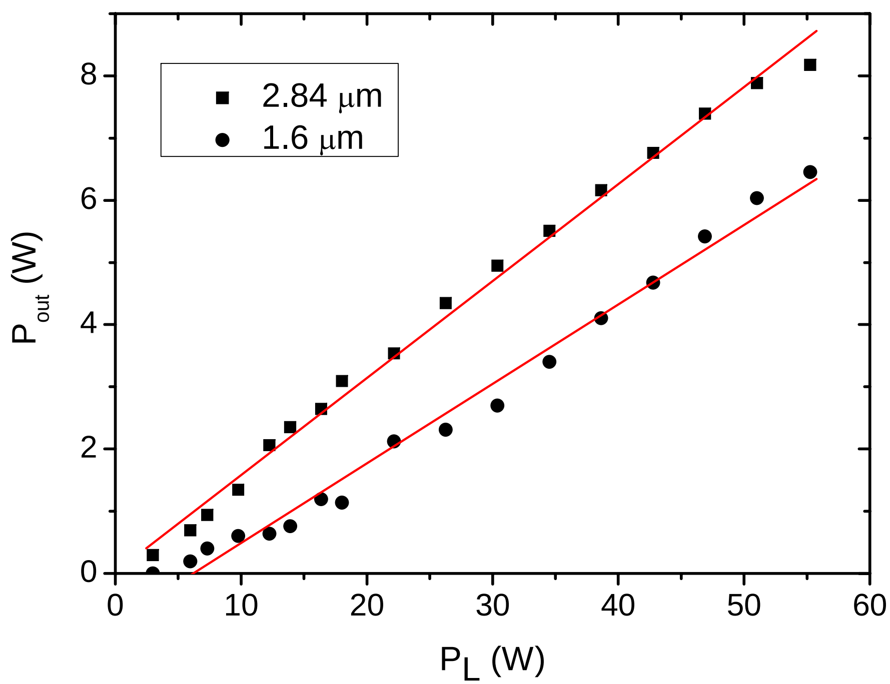

Calculated

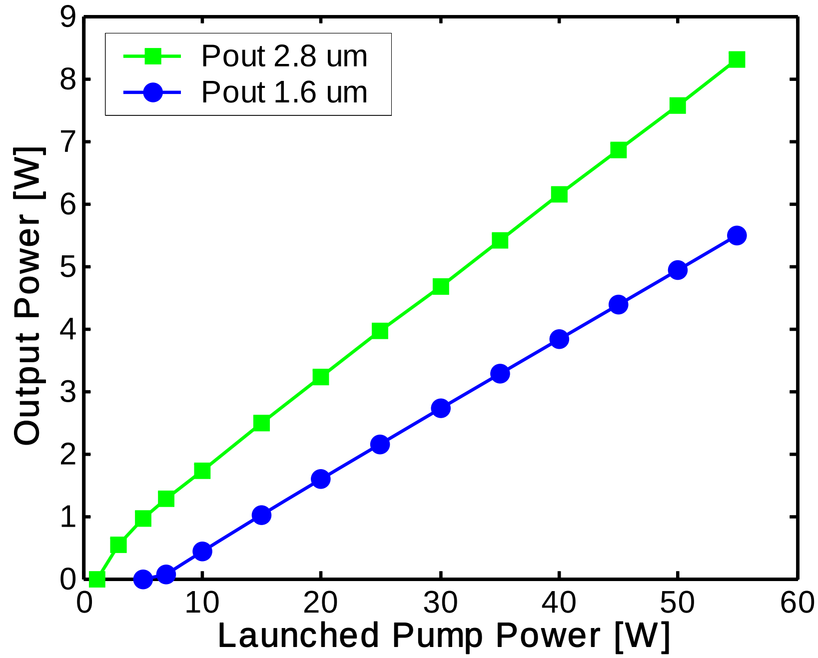

S.D. Jackson et al., submitted (2010)

Population Densities and Heat Input

Calculated population densities

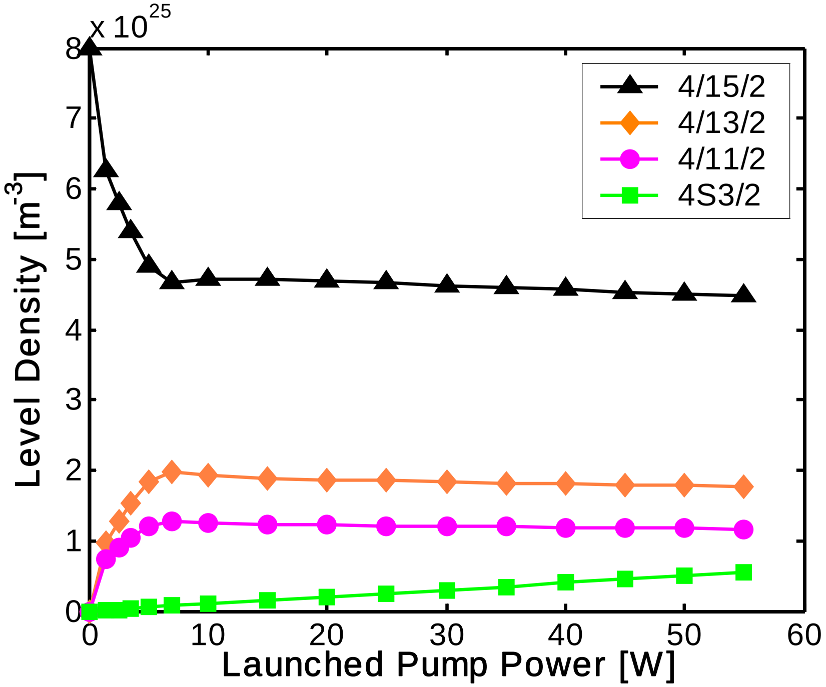

Calculated heat input

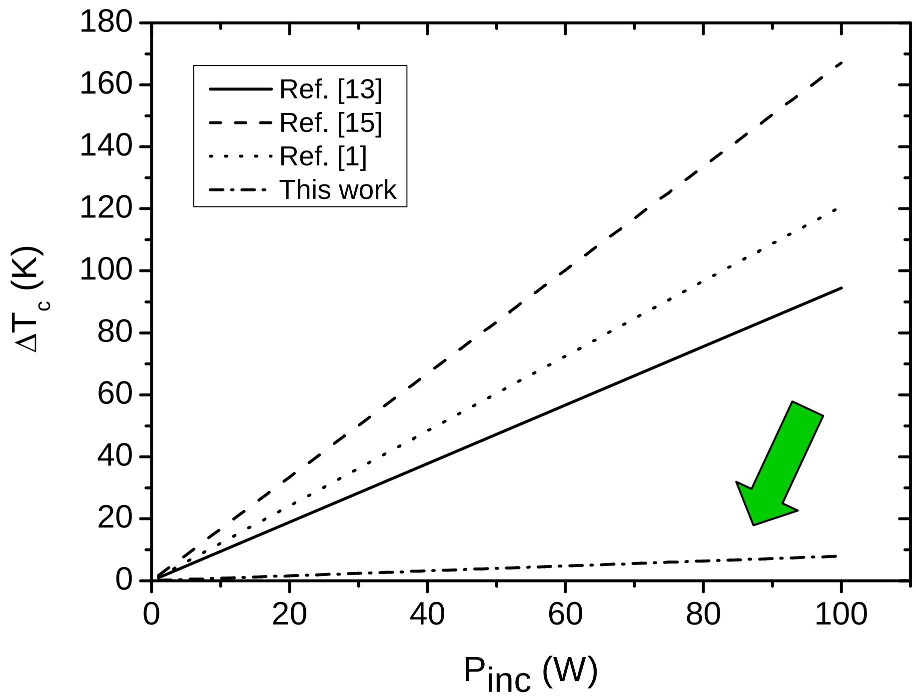

Concerning heat input, there's plenty of room for higher power!

S.D. Jackson et al., submitted (2010)

Latest Experimental Result

Uncooled ZBLAN fiber doped with 6 mol% Er^{3+}

9 W output power with 21% slope efficiency.

X.S. Zhu et al., Opt. Lett. 32 (2007) 26

Cooled ZBLAN fiber doped with 6 mol% Er^{3+}

24 W output power with 16% slope efficiency.

S. Tokita et al., Opt. Lett. 34 (2009) 3062

Uncooled ZBLAN fiber doped with 0.5 mol% Er^{3+}

8 W output power with 19% slope efficiency, cascade laser.

S.D. Jackson et al., submitted (2010)

Other 3-μm Fiber Lasers

T. Sumiyoshi,
"High-power continuous-wave 3- and 2-μm cascade Ho^{3+}:ZBLAN fiber laser and its medical applications",
IEEE J. Select. Topics Quantum Electron. 5 (1999) 936

S.D. Jackson,
"Single-transverse-mode 2.5 W holmium-doped fluoride fiber laser operating at 2.86 μm",
Opt. Lett. 29 (2004) 334

S.D. Jackson,
"Continuous wave 2.9 μm dysprosium-doped fluoride fiber laser",
Appl. Phys. Lett. 83 (2003) 1316

Summary

Population mechanisms of Er^{3+} 3-µm fiber laser depend on Er^{3+} conc., pump parameters, fiber geometry

$\Rightarrow$ we need to understand its spectroscopy!

With increasing erbium conc., four different operation regimes have successfully been demonstrated experimentally:

1. core pump, ESA $\Rightarrow$ upper cascade lasing
2. clad pump, codoping $\Rightarrow$ lifetime quenching
3. clad pump, ETU $\Rightarrow$ energy recycling
4. clad pump, laser depletion $\Rightarrow$ lower cascade lasing

Current output power is at 9 W uncooled and 24 W cooled.